

doi: 10.12097/gbc.2024.01.010

拉萨地块扎杠地区晚寒武世—早奥陶世流纹岩锆石U-Pb定年、岩石成因及其对原特提斯洋俯冲的启示

陈红灿¹,解超明^{1,2,3*},张家俊¹,白希泰¹,段梦龙¹

CHEN Hongcan¹, XIE Chaoming^{1,2,3*}, ZHANG Jiajun¹, BAI Xitai¹, DUAN Menglong¹

1. 吉林大学地球科学学院,吉林长春130061;

2. 东北亚矿产资源评价自然资源部重点实验室,吉林长春130061;

3. 吉林大学青藏高原地质研究中心,吉林长春130061

1. College of Earth Science, Jilin University, Changchun 130061, Jilin, China;

2. Key Laboratory of Mineral Resources Evaluation in Northeast Asia, Ministry of Land and Resources of China, Changchun 130061, Jilin, China;

3. Research Center for Qinghai-Tibetan Plateau, Jilin University, Changchun 130061, Jilin, China

摘要:【研究目的】青藏高原南部早古生代岩浆作用对于揭示冈瓦纳大陆北缘的大陆边缘性质及原特提斯洋的俯冲过程具有重要的研究意义,通过对拉萨地块申扎县北部扎杠地区发现的晚寒武世—早奥陶世流纹岩进行研究,探讨该流纹岩的岩石成因及地质意义,为进一步约束申扎地区扎杠不整合时限,并为认识冈瓦纳大陆北缘在早古生代的地质演化过程提供依据。

【研究方法】对青藏高原北拉萨地块申扎县北部扎杠地区流纹岩的LA-ICP-MS锆石U-Pb年龄、锆石Hf同位素及地球化学进行研究。**【研究结果】**流纹岩的锆石 $^{206}\text{Pb}/^{238}\text{U}$ 年龄加权平均值为 485 ± 5 Ma,样品显示出高硅、富碱、富铝、低磷、低镁等地球化学特征, SiO_2 含量为75.10%~77.39%, Al_2O_3 含量为10.74%~12.90%, $\text{K}_2\text{O}+\text{Na}_2\text{O}$ 为6.65%~7.99%, P_2O_5 含量介于0.03%~0.11%之间, MgO 含量为0.27%~0.35%, A/CNK 值为1.20~1.61,大于1.1,为强过铝质钾玄岩岩石系列。扎杠流纹岩表现出轻稀土元素富集,重稀土元素元素相对平坦的特征,有较明显的轻、重稀土元素分馏,并伴随强烈的负Eu异常($\delta\text{Eu}=0.44\sim0.48$),扎杠流纹岩具有较高的Rb($368.43\times10^{-6}\sim489.42\times10^{-6}$)含量, $\text{Zr/Hf}(31.97\sim37.35)$ 、 $\text{Nb/Ta}(12.17\sim15.32)$ 值较低,指示其在形成过程中发生了强烈的结晶分异作用,在 $\text{SiO}_2\text{--Zr}$ 图解及ACF图解中,样品落入S型花岗岩区域,显示出高分异S型花岗岩的特征;锆石 $\varepsilon_{\text{Hf}}(t)$ 值变化范围较小,介于-2.0~5.5之间,平均为-3.7,均为负值,指示其可能是地壳部分熔融的产物,Hf同位素二阶段模式年龄为1581~1752 Ma,表明中元古代地壳物质可能为其岩浆源区。**【结论】**综合前人研究资料及样品特征,扎杠地区晚寒武世—早奥陶世流纹岩可能形成于原特提斯洋洋壳向冈瓦纳大陆北缘俯冲的构造背景之下。

关键词:青藏高原;扎杠地区;流纹岩;地球化学;锆石U-Pb年龄

创新点:(1)为认识冈瓦纳大陆北缘在早古生代的地质演化过程提供依据,补充地质资料;(2)进一步约束了申扎地区扎杠不整合的时限为早奥陶世早期。

中图分类号:P534.4; P588.14⁺¹; P597.3 文献标志码:A 文章编号:1671-2552(2025)02/03-0441-18

Chen H C, Xie C M, Zhang J J, Bai X T, Duan M L. Zircon U-Pb age, petrogenesis and the revelation to the Proto-Tethyan ocean of the Late Cambrian-Early Ordovician rhyolite from Zhakang area in the Lhasa terrane. *Geological Bulletin of China*, 2025, 44(2/3): 441-458

Abstract: [Objective] The Early Paleozoic magmatism in the southern Qinghai-Tibet Plateau is important for researching the nature of the continental margin of the northern margin of the Gondwana continent and the subduction process of the Proto-Tethys Ocean.

收稿日期:2024-01-08;修订日期:2024-04-13

资助项目:国家自然科学基金项目《唐加-松多蛇绿岩及对青藏高原古特提斯洋演化制约》(批准号:42172226)

作者简介:陈红灿(1999-),男,在读硕士生,地质学专业。E-mail: 1721617920@qq.com

*通信作者:解超明(1983-),男,教授,从事构造地质学研究。E-mail: xcmxcm1983@jlu.edu.cn

Based on the research of the Late Cambrian–Early Ordovician rhyolite found in the Zhakang area in the northern part of Xainza County, Lhasa block, this paper discusses the petrogenesis and geological significance of the rhyolite, so as to further constrain the time limit of the Zhakang unconformity in the Xainza area, and provide a basis for understanding the geological evolution process of the northern margin of the Gondwana continent in the Early Paleozoic. [Methods] In this study, we report the zircon U–Pb age, rock geochemistry and zircon Hf isotope analysis of rhyolites in Zhakang area, northern Xainza County, Lhasa Block, Qinghai–Tibet Plateau. [Results] The results show that the weighted average age of zircon $^{206}\text{Pb}/^{238}\text{U}$ of rhyolite is 485 ± 5 Ma. The rock geochemistry shows high silicon, rich alkali, rich aluminum, low phosphorus and low magnesium. The content of SiO_2 is 75.10%~77.39%, the content of Al_2O_3 is 10.74%~12.90%, the content of $\text{K}_2\text{O}+\text{Na}_2\text{O}$ is 6.65%~7.99%, the content of P_2O_5 is 0.03%~0.11%, the content of MgO is 0.27%~0.35% and the A/CNK is 1.20~1.61, which is greater than 1.1. It belongs to a set of strongly peraluminous shoshonite series. The character in rare earth elements of the rhyolite is enrichment of light rare earth elements and relatively flat right-inclined curve of heavy rare earth elements. The fractionation of light and heavy rare earth elements is obvious, accompanied by obvious negative Eu anomalies ($\delta\text{Eu}=0.44\sim 0.48$). The Zhakang rhyolite has high Rb ($368.43\times 10^{-6}\sim 489.42\times 10^{-6}$) content, low Zr/Hf (31.97~37.35) and Nb/Ta (12.17~15.32) values, indicating that strong crystallization differentiation occurred during its formation. In the SiO_2 –Zr diagram and ACF diagram, the samples fell into the S-type granite area, showing the characteristics of highly differentiated S-type granite. The $\varepsilon_{\text{Hf}}(t)$ value of zircon varies from -2.0 to -5.5, with an average of -3.7, which is negative, indicating the rhyolite might be the product of partial melting of the crust. The two-stage model age of Hf isotope is 1581~1752 Ma, indicating that the source area may be Mesoproterozoic crustal material. [Conclusions] This study believes that the Late Cambrian–Early Ordovician rhyolite in the Zhakang area may be formed under the tectonic background of the subduction of the proto-Tethys oceanic crust to the northern margin of the Gondwana continent.

Key words: Qinghai-Tibet Plateau; Zhakang area; rhyolites; geochemistry; zircon U–Pb age

Highlights: (1) To provide a basis for understanding the geological evolution process of the northern margin of the Gondwana continent in the Early Paleozoic, and to supplement geological data; (2) It is further constrained that the time limit of the Zhakang unconformity in the Xianza area is the early Early Ordovician.

新元古代晚期—早古生代是冈瓦纳大陆拼合和周缘原特提斯洋俯冲造山的重要时期(Meert, 2003; Collins and Pisaresky, 2005; Cawood and Buchan, 2007; Cawood et al., 2007; Murphy et al., 2011)。现有研究表明,冈瓦纳大陆北缘经历了早古生代的造山作用,且发育有大量早古生代的岩浆岩(Gehrels et al., 2006; Cawood et al., 2007; 董昕等, 2009; Zhu et al., 2012; Hu et al., 2013; Ding et al., 2015)。对于这些早古生代的岩浆成因,仍存有争议,主要存在以下4种不同解释:①这些岩浆事件属于泛非期—早古生代造山运动的结果(许志琴等, 2005; 李才等, 2010);②可能是早古生代时期,在冈瓦纳大陆北缘,原特提斯洋洋壳发生俯冲导致的安第斯型岩浆活动(Cawood et al., 2007; Zhu et al., 2012; Zhang et al., 2014; 解超明等, 2021);③可能形成于后碰撞伸展拆离环境(Liu et al., 2009; Li et al., 2016; 张天羽, 2018; Liu et al., 2019, 2020);④这些分布在冈瓦纳大陆北缘的早古生代花岗岩可能是一个潜在的硅质大火成岩省遗迹(Dan et al., 2022)。

青藏高原中南部北拉萨地块,是冈瓦纳大陆北

缘的一部分,对解决上述争议具有重要的约束意义。北拉萨地块申扎地区的奥陶系与寒武系之间的角度不整合是目前在青藏高原中南部地区发现的时代依据及地层信息保存最充分的不整合(李才等, 2010; 张天羽, 2018)。在拉萨地块,上覆的下奥陶统扎拉组与下伏寒武系扎欠群以近90°的角度不整合相交(李才等, 2010),依据扎欠群中流纹岩的年龄,将晚寒武世—早奥陶世暂定为该不整合的形成时代(计文化等, 2009; 李才等, 2010; 张天羽, 2018)。然而,申扎地区这套不整合时代及早古生代的构造演化历史仍没有得到很好的约束,其成因与构造背景也一直存有争议。

因此,本文通过对拉萨地块申扎县北部扎拉地区发现的晚寒武世—早奥陶世流纹岩进行全岩地球化学、年代学研究,探讨该流纹岩的岩石成因及地质意义,为进一步约束申扎地区扎拉不整合时限,并为认识冈瓦纳大陆北缘在早古生代的地质演化过程提供依据。

1 地质概况及样品特征

青藏高原南部被一系列近东西向展布的板块缝

合带分割,自北向南分别为龙木错-双湖-澜沧江-昌宁-孟连缝合带(李才, 2008; 王保弟等, 2018)、班公湖-怒江缝合带(Pan et al., 2012; Zhu et al., 2016; 范建军等, 2018)和雅鲁藏布江缝合带(吴福元等, 2014; Liu et al., 2016)。拉萨地块位于青藏高原中南部,夹持于北部的班公湖-怒江缝合带与南部的印度-雅鲁藏布江缝合带之间(Allègre et al., 1984; Zhu et al., 2009)。Zhu et al.(2011, 2013)以狮泉河-纳木错蛇绿混杂岩带、唐加-松多缝合带为界,将拉萨地块自北向南划分为北、中、南三部分。而本文主要关注早古生代原特提斯洋与冈瓦纳大陆北缘的构造演化过

程,因此采用Yang et al.(2009)和Chen et al.(2009)以唐加-松多缝合带(洛巴堆-米拉山断裂带)为界线将拉萨地块划分为南拉萨地块及北拉萨地块的划分方案。

研究区大地构造位置处于北拉萨地体中部(图1-b),出露地层由下至上分别为中寒武统扎欠群(C_2z)、下奥陶统扎扛组(O_1z)、中奥陶统科尔多组(O_2k)、上奥陶统刚木桑组(O_3g)、志留系(S)、下泥盆统达尔东组(D_1d)、下泥盆统下石炭统查果罗马组(D_1C_1c)、下石炭统永珠组(C_1y)及第四系沉积物(Q)。上覆下奥陶统与下伏寒武系之间为角度不整

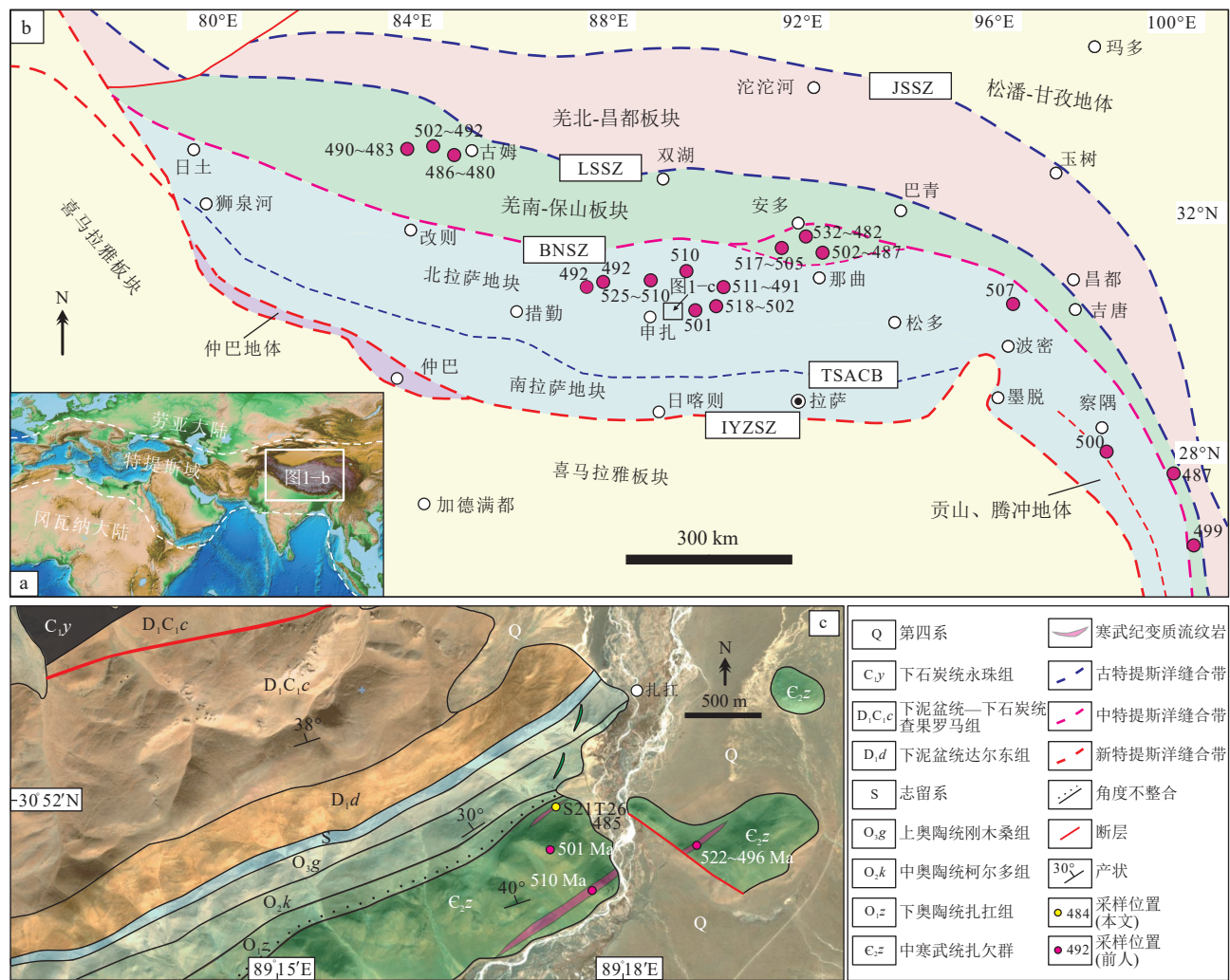


图1 特提斯域地形图(底图下载于 <http://www.ngdc.noaa.gov/mgg/global/>) (a)、青藏高原中部构造划分图 (b, 年龄单位 Ma) 和
申扎地区扎扛一带地质简图 (c)(据 Xu et al., 2015 修改)(图中年龄见表 4)

Fig. 1 Tethyan realm, topographic map (a), simplified tectonic map of the central Tibetan Plateau (b) and
geological map of the Zhakang area in Xainza (c)

JSSZ—金沙江缝合带; LSSZ—龙木错-双湖-澜沧江缝合带; BNSZ—班公湖-怒江缝合带; TSACB—唐加-松多蛇绿混杂岩带;
IYZSZ—雅鲁藏布江缝合带(据董宇超, 2021)

合接触, 奥陶系—石炭系为连续的古生代沉积地层(丁慧霞, 2015)。

扎欠群从下到上依次为粉砂质泥岩、酸性熔结凝灰岩、泥岩、流纹岩、长石石英砂岩、粉砂岩, 由以火山岩为主的地层组成, 反映其处于活动大陆边缘环境(计文化等, 2009)。扎杠组主要由变质的泥质粉砂岩、细砂岩夹结晶灰岩组成; 科尔多组主要岩性为薄层—厚层微晶泥晶灰岩; 刚木桑组为一套中薄层泥晶灰岩、泥质条带灰岩夹粉系砂岩; 志留系主要岩性为灰岩、粉细砂岩; 达尔东组主要岩性为中薄层微晶灰岩, 偶夹砂屑灰岩; 查果罗马组为一套中厚—巨厚层状泥晶灰岩; 永珠组主要岩性为灰绿色细砂岩夹细粒石英砂岩(程立人等, 2005; 刘志强, 2006)。

本文报道的流纹岩出露于申扎县买巴乡东南约40 km 的扎杠一带(图 1-c), 出露于扎欠群的上部层位, 流纹岩风化面呈黄褐色, 新鲜面为灰黑色, 似斑状结构, 流动构造(图 2), 斑晶(25%~30%)和基质(75%~70%)均由长石类矿物及石英组成。斑晶为石英和钾长石。石英呈自形—半自形粒状, 表面干净光滑, 干涉色为一级灰白, 粒径为2~5 mm, 具波状消光; 钾长石呈半自形—他形短柱状, 干涉色为一级灰白, 粒径2~4 mm, 基质主要由霏细状石英和长石组

成。镜下可见明显的流纹构造(图 2-d)。

2 样品测试方法

2.1 锆石 U-Pb 定年

本文对扎杠地区流纹岩样品(S21T26)进行了锆石 U-Pb 年龄测定, 在河北省廊坊市(宇能)宇恒矿岩技术服务有限公司对测试的样品锆石进行常规方法分选、锆石制靶、阴极发光照相等工作(段梦龙等, 2022)。用于 LA-ICP-MS 测试及阴极发光分析的锆石颗粒先在双目镜下挑选出干净透明、无裂隙和包裹体的颗粒, 随后置于环氧树脂中, 并磨至约1/2, 使其内部暴露(解超明等, 2010)。在吉林大学东北亚矿产资源评价自然资源部重点实验室进行锆石 LA-ICP-MS 原位分析, 以阴极发光(CL)图像所显示的锆石内部结构作为依据。使用的 ICP-MS 为 Agilent 7500a 型, 激光剥蚀系统为 UP193SS 型、深紫外(DUV)193 nm、ArF 准分子激光剥蚀系统, 激光束斑直径为 36 μm。实验中采用载气 He, 流速 0.7 L/min, 在同位素比值校正时, 外标为标准锆石 91500, 监控盲样为标准锆石 TEM(417 Ma); 以 NIST610 国际标样为外标、Si 为内标对元素含量进行计算, 监控盲样为 NIST612 和 NIST614。同位素比值采用 Glitter4.4 软件进行处理, 锆石 U-Pb 年龄

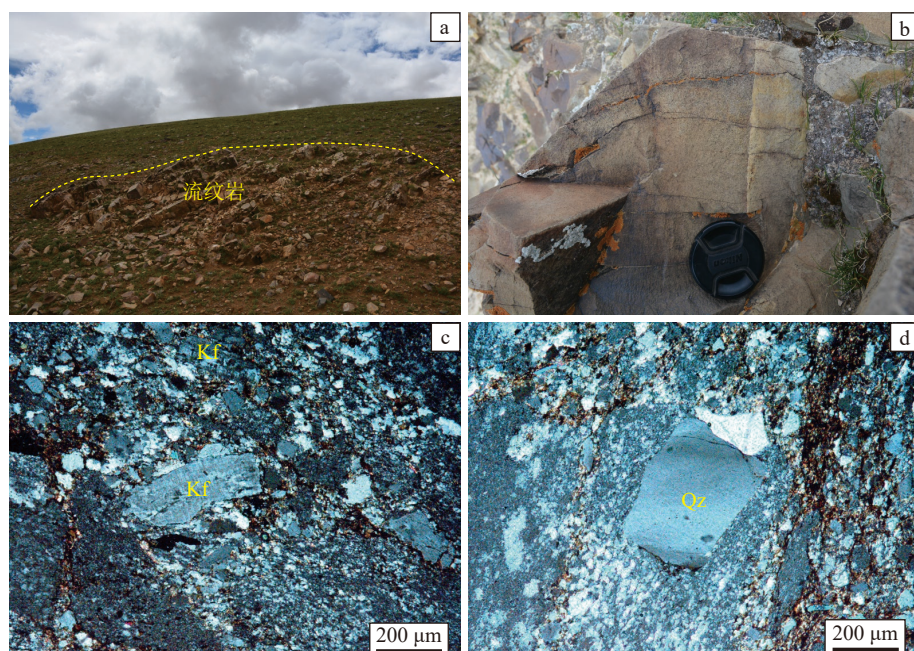


图 2 扎杠地区晚寒武世—早奥陶世流纹岩野外露头照片(a, b)和显微镜下正交偏光照片(c, d)

Fig. 2 Field characteristics(a, b) and micrographs(c, d)of the Late Cambrian–Early Ordovician rhyolite from Zhakang area
Qz—石英; Kf—钾长石

加权平均值及绘制年龄谐和图用 Isoplot 程序进行计算和绘制(解超明等, 2014; 张雨轩等, 2018; 罗安波, 2022)。

2.2 锆石 Hf 同位素测试

在北京科荟测试技术有限公司实验室对锆石 Hf 同位素进行测试时, 利用激光剥蚀多接收器电感耦合等离子体质谱仪来完成。在温度 18~22°C, 相对湿度<65% 的外界检测环境下, 以 NWR213 nm 固体激光器为激光进样系统, 多接收等离子体质谱仪(NEPTUNE plus)为分析系统, 仪器的具体运行条件及相关分析方法详见文献(Hu et al., 2012)。在对锆石进行剥蚀时采用 NWR213 nm 固体激光器, 剥蚀的激光束斑直径为 40 μm, 能量密度为 10~11 J/cm², 频率为 10 Hz, 以高纯氦为载气把激光剥蚀的物质送入 Neptune Plus (MC-ICPMS), 接收器配置与溶液进样方式相同。采用软件 ICPMSData Cal 对样品、空白信号的选择及同位素质量分馏进行校正(Liu et al., 2010; 张雨轩等, 2018)。

2.3 全岩地球化学分析

在河北廊坊市(宇能)宇恒矿岩技术服务有限公司利用无污染碎样机将岩石样品精碎至小于 5 mm 左右, 再将其在无污染玛瑙球磨机下磨至 200 目, 后送往地球化学分析实验室备用。地球化学样品的主量、微量元素和稀土元素分析均在北京科荟测试技术有

限公司完成(解超明等, 2019)。主量元素采用 X-射线荧光光谱仪(SHIMADZU XRF-1800)分析。微量元素和稀土元素的分析仪器为 Analyticjena PQMS elite 等离子质谱仪, 实验室分析方法详见参考文献(Hu et al., 2019; 吴昊等, 2021)。

3 测试结果

3.1 锆石 U-Pb 定年

本文获得 13 个较好的锆石 U-Pb 同位素数据(表 1)。岩浆振荡环带结构在该样品锆石中较典型(图 3-a), 有较完整的晶形, 呈半自形—自形, 长 50~200 μm, 长/宽为 1:2~1:3, 锆石的稀土元素(REE)含量高, 为 764×10⁻⁶~3786×10⁻⁶, 在锆石稀土元素配分图(图 3-a)中, 表现出轻稀土元素(LREE)亏损, 重稀土元素(HREE)相对富集的特征, 并有显著的正 Ce 异常及负 Eu 异常, 与前人报道的扎扛变质流纹岩的特征相似(Hu et al., 2013)。锆石测点的 Th 含量为 224×10⁻⁶~1109×10⁻⁶, U 为 316×10⁻⁶~750×10⁻⁶, Th/U 值介于 0.70~1.48 之间(表 2), 均大于 0.1。以上特点表明, 参与计算的测点对应锆石为岩浆成因。

在年龄谐和图(图 3-b)上, 所有锆石测点的年龄数据均在谐和线上及其附近, 其²⁰⁶Pb/²³⁸U 年龄加权平均值为 485±5 Ma, 代表了锆石的结晶年龄, 表明

表 1 扎扛晚寒武世—早奥陶世流纹岩锆石 U-Th-Pb 同位素测年数据

Table 1 U-Th-Pb isotope composition of the zircons in the Late Cambrian-Early Ordovician rhyolite from the Zhakang as measured by LA-ICP-MS

点号	含量/10 ⁻⁶			Th/U	同位素比值						年龄/Ma					
	Pb	Th	U		²⁰⁷ Pb/ ²⁰⁶ Pb 1σ	²⁰⁷ Pb/ ²³⁵ U 1σ	²⁰⁶ Pb/ ²³⁸ U 1σ	²⁰⁷ Pb/ ²⁰⁶ Pb 1σ	²⁰⁷ Pb/ ²³⁵ U 1σ	²⁰⁶ Pb/ ²³⁸ U 1σ	²⁰⁷ Pb/ ²⁰⁶ Pb 1σ	²⁰⁷ Pb/ ²³⁵ U 1σ	²⁰⁶ Pb/ ²³⁸ U 1σ			
01	69	599	639	0.94	0.0569	0.0041	0.6304	0.0558	0.0777	0.0013	487	168	496	35	482	8
02	36	266	344	0.78	0.0558	0.0026	0.6219	0.0291	0.0797	0.0016	443	68	491	18	495	10
03	98	1109	750	1.48	0.0559	0.0025	0.6029	0.0267	0.0769	0.0012	447	71	479	17	478	7
04	70	649	612	1.06	0.0559	0.0022	0.6088	0.0218	0.0784	0.0014	446	48	483	14	487	8
05	68	729	575	1.27	0.0559	0.0019	0.5951	0.0201	0.0766	0.0013	447	45	474	13	476	8
06	37	260	325	0.80	0.0567	0.0019	0.6119	0.0215	0.0783	0.0018	480	39	485	14	486	11
07	55	424	512	0.83	0.0567	0.0024	0.6048	0.0264	0.0774	0.0019	479	55	480	17	481	11
08	39	276	334	0.83	0.0567	0.0022	0.6147	0.0247	0.0786	0.0019	480	48	487	16	488	11
09	36	236	316	0.75	0.0568	0.0019	0.6240	0.0212	0.0796	0.0019	485	37	492	13	494	11
10	45	364	432	0.84	0.0569	0.0071	0.6182	0.0759	0.0788	0.0029	486	207	489	48	489	18
11	59	460	478	0.96	0.0574	0.0017	0.6217	0.0192	0.0786	0.0019	506	32	491	12	488	11
12	39	224	322	0.70	0.0607	0.0036	0.6652	0.0388	0.0795	0.0021	628	80	518	24	493	13
13	39	269	337	0.80	0.0572	0.0023	0.6332	0.0262	0.0803	0.0020	498	49	498	16	498	12

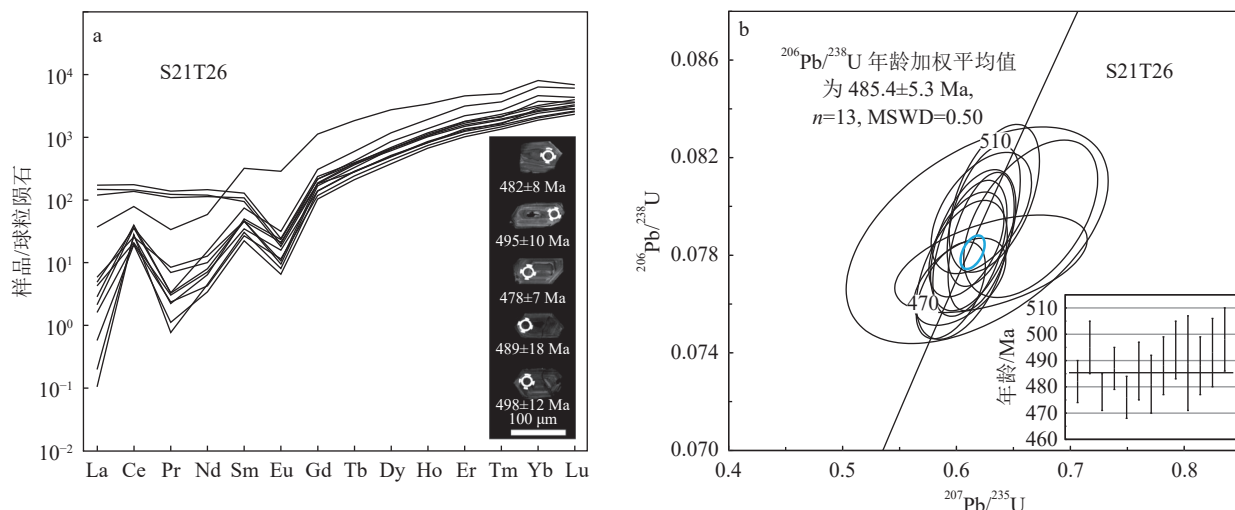


图3 扎扛流纹岩锆石稀土元素配分图、阴极发光(CL)图像(a)和锆石U-Pb谐和图(b)

Fig. 3 Rare earth element patterns and typical cathodoluminescence images (a) and U—Pb concordia diagram (b) of the zircons from the Late Cambrian—Early Ordovician rhyolite in Zhakang

表2 扎扛晚寒武世—早奥陶世流纹岩锆石Lu—Hf同位素测年数据

Table 2 Lu—Hf isotope composition of the zircons from the Late Cambrian—Early Ordovician rhyolite of the Zhakang

点号	$^{206}\text{Pb}/^{238}\text{U}$ 年龄/Ma	$^{176}\text{Yb}/^{177}\text{Hf}$	2σ	$^{176}\text{Lu}/^{177}\text{Hf}$	2σ	$^{176}\text{Hf}/^{177}\text{Hf}$	2σ	$(^{176}\text{Hf}/^{177}\text{Hf})_i$	$\varepsilon_{\text{Hf}}(0)$	$\varepsilon_{\text{Hf}}(t)$	2σ	T_{DM}/Ma	T_{DM2}/Ma	$f_{\text{Lu/Hf}}$
01	482	0.073226	0.004264	0.002471	0.000129	0.282437	0.000030	0.282415	-11.9	-2.0	1.1	1200	1581	-0.93
02	495	0.074632	0.000494	0.002546	0.000029	0.282420	0.000025	0.282396	-12.5	-2.4	0.9	1227	1614	-0.92
03	478	0.044091	0.000530	0.001413	0.000015	0.282380	0.000018	0.282367	-13.9	-3.8	0.6	1247	1691	-0.96
04	487	0.040264	0.000964	0.001307	0.000030	0.282349	0.000020	0.282337	-15.0	-4.7	0.7	1287	1752	-0.96
06	486	0.036370	0.000450	0.001180	0.000015	0.282366	0.000019	0.282355	-14.4	-4.1	0.7	1259	1712	-0.96
08	488	0.047731	0.001225	0.001563	0.000030	0.282403	0.000020	0.282389	-13.0	-2.8	0.7	1218	1635	-0.95
10	489	0.059668	0.000748	0.002092	0.000023	0.282380	0.000030	0.282361	-13.8	-3.8	1.1	1269	1696	-0.94
11	488	0.052471	0.001283	0.001831	0.000052	0.282383	0.000025	0.282367	-13.7	-3.6	0.9	1256	1685	-0.94
13	498	0.059641	0.003792	0.001810	0.000074	0.282357	0.000021	0.282340	-14.7	-4.3	0.7	1293	1738	-0.95

该流纹岩形成时代为晚寒武世—早奥陶世。此外，还存在年龄较老的锆石($1040\sim2488\text{ Ma}$)，属于继承锆石，可能是流纹岩岩浆上升过程中捕获的。

3.2 锆石 Hf 同位素

同一颗锆石中，在测定锆石 U—Pb 年龄测点的相同或邻近部位进行 Lu—Hf 同位素的测试与分析，测试结果见表 2。锆石 $^{176}\text{Lu}/^{177}\text{Hf}$ 介于 $0.001180\sim0.002546$ 之间，仅有 3 个测点大于 0.002，暗示这些锆石受放射性成因 Hf 积累的影响较小，所以本文测定的 $^{176}\text{Lu}/^{177}\text{Hf}$ 值可以代表锆石形成时的 $^{176}\text{Lu}/^{177}\text{Hf}$ 值(吴福元等, 2007; 解超明等, 2019)。该流纹岩中锆石的 $\varepsilon_{\text{Hf}}(t)$ 值介于 $-2.0\sim-4.7$ 之间，平均值为 -3.5 ，二阶段 Hf 模式年龄(T_{DM2})为 $1581\sim1752\text{ Ma}$ ，平均值为 1678 Ma 。

3.3 全岩地球化学

流纹岩样品(S21T26)的全岩地球化学分析结果见表 3，样品烧失量较小($0.67\%\sim1.37\%$)，去烧失量处理之后， SiO_2 含量为 $75.87\%\sim78.78\%$ ，属于高硅流纹岩系列， Al_2O_3 含量为 $10.84\%\sim13.11\%$ ， $\text{K}_2\text{O}+\text{Na}_2\text{O}$ 含量为 $6.65\%\sim7.99\%$ ， CaO 为 $0.06\%\sim0.20\%$ ， TiO_2 为 $0.16\%\sim0.53\%$ ， P_2O_5 为 $0.03\%\sim0.11\%$ 。在 $\text{Nb}/\text{Y}-\text{Zr}/\text{TiO}_2\times0.0001$ 图解中，5 个样品点均落于流纹岩及流纹岩与英安岩过渡区域(图 4-a)。在 Co-Th 图解(图 4-b)上，样品点落入钾玄岩和高钾钙碱性区域；样品具有较高的 A/CNK 指数($1.20\sim1.61$ ，平均为 1.42)(>1.1)，在 A/CNK-A/NK 图解(图 4-c)上，样品点集中于过铝质区域，而在 $\text{SiO}_2-\text{K}_2\text{O}$ 图解(图 4-d)上，样品点落于钾玄岩系列区域。综合上述

表3 扎扛地区晚寒武世—早奥陶世流纹岩主量、微量元素和稀土元素含量

Table 3 Concentrations of major, trace elements and REE of the Late Cambrian—Early Ordovician rhyolite from the Zhakang area

元素	S21T26H1	S21T26H2	S21T26H3	S21T26H4	S21T26H5	元素	S21T26H1	S21T26H2	S21T26H3	S21T26H4	S21T26H5
SiO ₂	75.59	76.31	75.10	75.11	77.39	Y	21.58	34.19	27.42	35.09	32.39
TiO ₂	0.53	0.16	0.48	0.16	0.20	Zr	358.29	239.46	385.99	220.78	275.92
Al ₂ O ₃	10.74	12.38	10.92	12.90	11.85	Nb	13.48	14.93	16.93	15.19	16.95
TFe ₂ O ₃	3.69	1.87	3.84	1.98	1.77	Mo	0.51	0.49	0.30	0.05	0.04
TFeO	3.32	1.68	3.45	1.78	1.59	Sn	2.25	6.29	3.60	6.10	11.80
MnO	0.02	0.02	0.02	0.02	0.01	Cs	21.82	5.05	36.91	4.88	5.31
MgO	0.34	0.35	0.34	0.35	0.27	Ba	787.77	1203.55	940.69	1273.08	980.40
CaO	0.20	0.07	0.18	0.06	0.07	La	29.43	29.85	33.98	42.56	26.35
Na ₂ O	0.12	0.07	0.09	0.07	0.07	Ce	71.32	77.77	90.60	97.65	47.34
K ₂ O	7.75	7.14	7.90	7.65	6.58	Pr	6.63	6.80	7.60	9.60	6.46
P ₂ O ₅	0.11	0.03	0.11	0.03	0.03	Nd	23.18	24.41	26.53	34.69	23.71
烧失量	0.71	1.30	0.67	1.35	1.37	Sm	4.71	5.24	5.30	6.82	5.13
总计	99.79	99.70	99.65	99.69	99.61	Eu	0.65	0.77	0.78	1.00	0.69
A/CNK	1.20	1.56	1.21	1.51	1.61	Gd	3.95	5.00	4.66	6.32	4.53
A/NK	1.25	1.58	1.25	1.53	1.64	Tb	0.66	0.92	0.79	1.01	0.79
ALK	7.94	7.32	8.08	7.86	6.77	Dy	3.94	5.94	4.87	6.02	5.21
AI(NK/A)	0.80	0.63	0.80	0.65	0.61	Ho	0.82	1.27	1.02	1.26	1.17
σ	1.89	1.55	1.98	1.85	1.28	Er	2.39	3.71	2.93	3.73	3.74
DI	90.81	91.40	90.58	91.34	91.69	Tm	0.36	0.56	0.45	0.57	0.61
Mg [#]	17.9	30.3	17.3	29.0	26.3	Yb	2.37	3.61	2.88	3.72	4.19
Li	19.26	6.47	24.93	7.04	7.17	Lu	0.38	0.55	0.45	0.57	0.69
Be	1.30	2.05	1.51	2.07	1.74	Hf	9.92	6.99	10.62	6.46	8.63
Sc	5.51	3.81	6.49	3.95	4.34	Ta	0.88	1.23	1.14	1.23	1.26
Ti	2657.37	859.05	2655.12	850.87	1034.59	W	5.13	1.94	5.41	1.86	3.13
V	13.28	4.71	17.71	4.79	7.57	Tl	2.54	1.76	3.37	1.76	1.61
Cr	41.58	2.31	23.14	1.79	0.96	Pb	22.50	24.89	25.91	24.25	7.32
Mn	103.99	132.45	128.44	126.94	108.30	Th	32.44	24.29	34.01	20.78	28.85
Co	2.20	1.63	2.57	1.53	0.89	U	2.98	3.00	3.31	2.85	2.87
Ni	15.14	3.13	5.82	2.80	2.44	ΣREE	150.78	166.41	182.84	215.53	130.60
Cu	10.55	4.17	14.44	4.33	4.67	LREE	135.91	144.85	164.80	192.32	109.69
Zn	57.32	31.56	76.96	31.54	28.89	HREE	14.87	21.55	18.04	23.20	20.92
Ga	9.87	16.25	12.64	17.24	20.18	LREE/HREE	9.14	6.72	9.13	8.29	5.24
Rb	368.43	386.90	489.42	399.91	374.10	Eu/Eu [*]	0.46	0.46	0.48	0.47	0.44
Sr	15.20	18.54	18.68	19.64	13.79	(La/Yb) _N	8.91	5.94	8.47	8.20	4.52

注: 主量元素含量单位为%, 微量和稀土元素含量单位为10⁻⁶

特征,该流纹岩属于一套过铝质钾玄岩系列岩石。

流纹岩的稀土元素总量(ΣREE)较低,介于150.8×10⁻⁶~215.5×10⁻⁶之间,在稀土元素球粒陨石标准化模式图(图5-a)上,所有样品的曲线一致性较好,为右倾的“V”字形,显示出轻稀土元素相对富集,

重稀土元素相对平坦的特征,轻、重稀土元素分馏较明显,LREE/HREE=5.24~9.14,平均为7.71。(La/Yb)_N值为4.52~8.91,并表现出明显的负Eu异常,Eu/Eu^{*}值为0.44~0.48,在图中有负Eu异常的“谷”,具有类似于地壳稀土元素的特征(Wedepohl et al., 1992)。

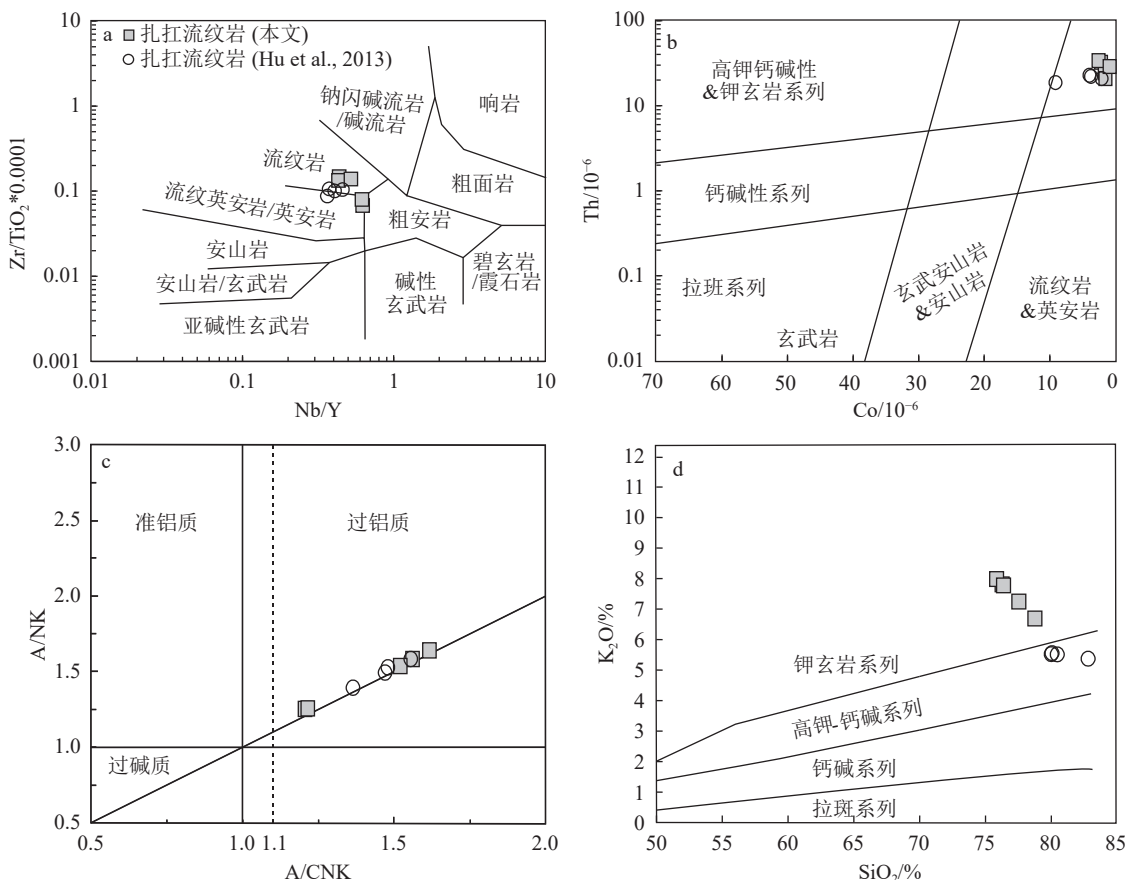


图4 扎杠地区晚寒武世—早奥陶世流纹岩 Nb/Y-Zr/TiO₂×0.0001(a, 底图据 Winchester and Floyd, 1977)、Co-Th(b, 底图据 Hastie et al., 2007)、A/CNK-A/NK(c, 底图据 Maniar and Piccoli, 1989)、SiO₂-K₂O(d, 底图据 Peccerillo and Taylor, 1976) 图解

Fig. 4 Nb/Y-Zr/TiO₂×0.0001(a), Co-Th(b), A/CNK-A/NK(c) and SiO₂-K₂O(d) diagrams of the Late Cambrian-Early Ordovician rhyolite from Zhakang area

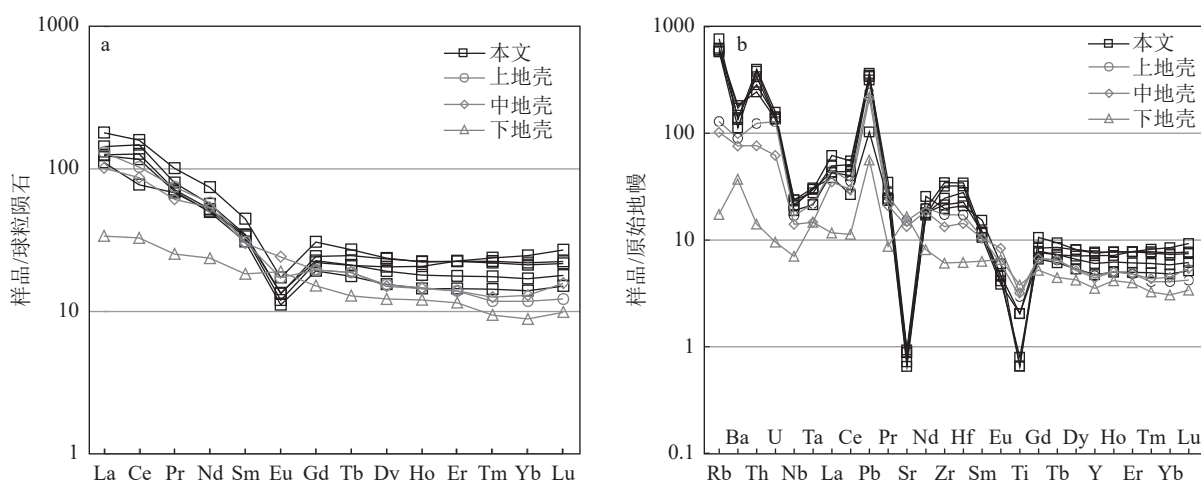


图5 扎杠地区晚寒武世—早奥陶世流纹岩球粒陨石标准化稀土元素配分图(a)和原始地幔标准化微量元素蛛网图(b)
 (标准化值据 Sun and McDonough, 1989; 地壳数据据 Wedepohl et al., 1995)

Fig. 5 Chondrite-normalized rare earth element patterns(a) and primitive mantle-normalized spider diagrams(b) for the Late Cambrian-Early Ordovician rhyolite from Zhakang area

al., 1995)。

在岩石微量元素蛛网图(图 5-b)中, 样品 Rb、Th、Pb 等元素明显富集, Nb、Ti、Ta、Sr 等高场强元素和 Ba 相对亏损, 类似于地壳熔融产生的流纹岩(刘一鸣等, 2014)。

4 讨 论

4.1 岩石类型

目前, 国内外学者对花岗岩的成因分类中, 普遍接受 MISA(即 M、I、S 和 A 型)的分类方案(徐文坦等, 2022)。当岩石的结晶分异程度较高时, 还可进一步划分出高分异 I 型和高分异 S 型花岗岩(Whalen et al., 1987; 张洪亮等, 2019)。但高分异花岗岩的类型, 往往需要通过矿物学及地球化学的综合分析进行判定。

扎扛流纹岩属于高硅流纹岩, SiO_2 含量为 75.87%~78.78%, 平均为 76.98%, 全碱含量 $\text{ALK}(\text{K}_2\text{O}+\text{Na}_2\text{O})$ 为 6.77%~8.08%, 铝过饱和指数 ($\text{A/CNK}=1.20\sim1.61$, 平均为 1.42) 较大, P_2O_5 (0.03%~0.11%, 平均为 0.06%)、 TiO_2 (0.16%~0.53%, 平均为 0.31%)、 MgO (0.28%~0.35%, 平均为 0.34) 含量都较低, 表现出低磷、低钛、低镁的特征, 结晶分异指数 (Df) 较高, 为 90.81~91.69; 同时, 在微量元素方面, 扎扛流纹岩表现出明显的负 Eu 异常 ($\delta\text{Eu}=0.44\sim0.48$), 大离子亲石元素(Rb、Th)和 Pb 等元素富集明显, 高场强元素(Nb、Ti、Ta、Sr)和 Ba 相对亏损, 富集 Th 而亏损 Ba, 轻、重稀土元素分馏明显, 在稀土元素配分模式图(图 5-a)中表现出轻稀土元素富集, 重稀土元素相对平坦的特征, 表明该流纹岩经历了结晶分异作用; 发生结晶分异作用的花岗质岩浆, 其 Li、Rb 等元素的含量与岩浆分异程度成正相关关系, 而 Cr、Ni、Sr、Ba 等元素的含量会随着分异程度的增加而降低, 岩浆中 Zr/Hf 、 Nb/Ta 等元素的比值也会随之增加而降低(Linnen and Keppler, 2002; Lee and Morton, 2015; 张洪亮等, 2019)。扎扛流纹岩具有较高的 Rb($368.43\times10^{-6}\sim489.42\times10^{-6}$) 含量, Zr/Hf (31.97~37.35)、 Nb/Ta (12.17~15.32) 值较低。综上所述, 扎扛流纹岩在向上喷涌时发生了强烈的结晶分异作用, 类似于高分异花岗岩。

在区分 I 型、S 型与 A 型花岗岩时, 采用 $\text{SiO}_2\text{-TFeO/MgO}$ 图解(图 6-a)效果较好。本文扎扛流纹岩样品投点落入 I&S 区域。同时, 结合以下几点原

因, 判定扎扛流纹岩为 S 型花岗岩: ①扎扛流纹岩的全碱含量 $\text{K}_2\text{O}+\text{Na}_2\text{O}$ 为 6.77%~8.08%, $\text{AI}(\text{NK/A})=0.61\sim0.80$, 小于 0.85, 与 S 型花岗岩对应(Whalen et al., 1987), $\text{A/CNK}=1.20\sim1.61$, 平均为 1.42, 大于 1.1, 与 S 型花岗岩吻合; ②该流纹岩具有明显的负 Eu 异常, δEu 平均值为 0.46, 不同于 I 型花岗岩(张洪亮等, 2019); ③在高分异 I 型花岗岩中, 其 TFeO 含量通常小于 1%(王强等, 2000; 徐文坦等, 2022), 本文流纹岩 TFeO 含量为 1.59%~3.32%, 与之不符; ④在 $\text{SiO}_2\text{-Zr}$ 图解及 ACF 图解(图 6-b, d)中, 所有样品点均落入 S 型花岗岩区域; ⑤对比本文流纹岩锆石微量元素特征与之前报道的 S 型扎扛流纹岩锆石微量元素特征(Hu et al., 2013), 二者十分相似(图 6-d), 均落入 S 型花岗岩区域, 指示扎扛流纹岩类似于 S 型花岗岩。综上所述, 扎扛流纹岩可能为高分异 S 型花岗岩。

4.2 岩浆演化及源区

扎扛流纹岩稀土元素配分曲线表现为右倾型, Rb 的富集、Ba 的亏损表明岩浆经历了结晶分异作用; 钛铁矿的分离结晶作用会造成 Ti 元素的亏损, 且能指示岩浆源区中含有地壳组分; Ba、Sr 的明显亏损及显著的负 Eu 异常指示岩浆可能发生了斜长石的分离结晶, 也暗示其可能是壳源物质发生低程度部分熔融形成的(Harris and Inger, 1992)。以上证据表明, 扎扛流纹岩在岩浆演化过程中可能经历了以钛铁矿和斜长石为主的分离结晶作用(李献华等, 2007)。

通常认为, 酸性火成岩成因可能包括: ①由幔源岩浆广泛的分离结晶而形成, 流纹质岩浆的形成可能有多种物质来源, 包括富地幔、贫地幔和长英质地壳(Civetta et al., 1998; Lustrino et al., 2000; Ronga et al., 2010); ②由幔源岩浆底侵引起的地壳部分熔融形成(Clemens, 2003; Kemp et al., 2006, 2008); ③幔源岩浆与壳源岩浆混合(张亮亮等, 2010; Chen et al., 2012)。沿冈瓦纳原特提斯边缘的早古生代酸性火成岩大部分是第二种成因(498~502 Ma, Liu et al., 2009; 488.6~517.9 Ma, 王晓先等, 2011; 492 Ma, Zhu et al., 2012; 511 Ma, Hu et al., 2013)。本文的流纹岩也是第二种成因, 原因如下: ①幔源岩浆的分离结晶形成的流纹岩通常伴随大量的中基性岩浆岩, 并且基性岩浆岩的分布面积最广(张博川, 2021)。然而, 在申扎地区目前并没有发现和报道同时期的基性岩

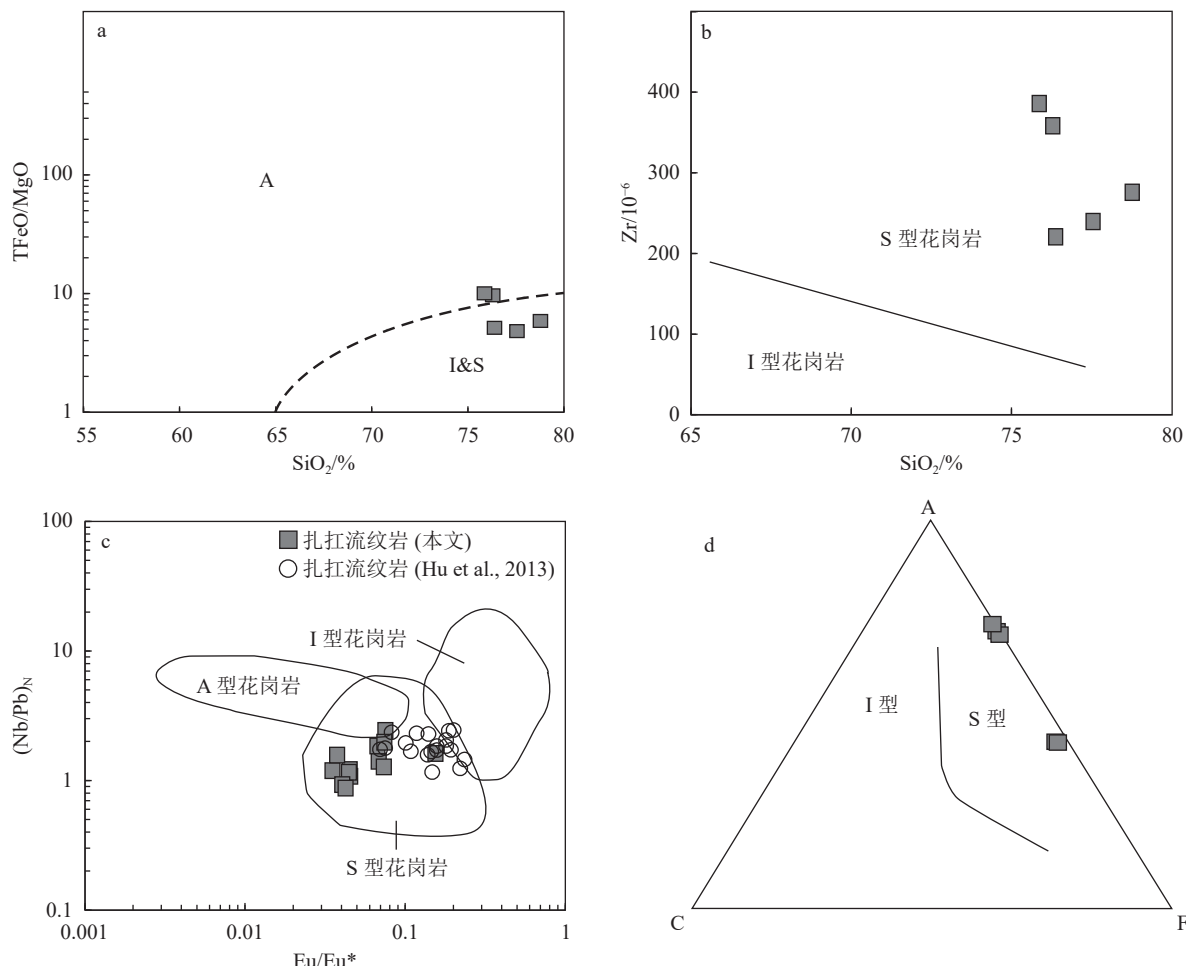


图 6 扎杠流纹岩 SiO_2 -TFeO/MgO(a, 底图据 Whalen et al., 1987)、 SiO_2 -Zr(b, 底图据 Watson and Harrison, 1983)、锆石 $\text{Eu}/\text{Eu}^*-(\text{Nb}/\text{Pb})_N$ (c, 底图据 Grimes et al., 2007) 和 ACF 图解(d, 底图据 Collins, 1982)

Fig. 6 SiO_2 -TFeO/MgO(a), SiO_2 -Zr (b), zircon $\text{Eu}/\text{Eu}^*-(\text{Nb}/\text{Pb})_N$ (c) and ACF (d) diagrams for the rhyolite from Zhakang and Blichert-Toft

(Hu et al., 2013),因此其并非由幔源岩浆分离结晶形成;②扎杠流纹岩 Rb/Sr、Ti/Y 和 Ti/Zr 值分别为 20.36~27.13(平均为 23.76, >0.5)、24.25~96.83(平均为 44.54, <100)、3.59~7.42(平均为 5.10, <20), 属于壳源岩浆(Pearce, 1983; Tischendorf and Paelchen, 1985; Wilson, 1989);③当 $\text{CaO}/\text{Na}_2\text{O}>0.3$ 时, 过铝质花岗岩可能由杂砂岩熔融形成, 扎杠流纹岩的 $\text{CaO}/\text{Na}_2\text{O}$ 值平均为 1.28, 指示其源岩可能为杂砂岩(Jung and Pfander, 2007), 而在 Rb/Sr-Rb/Ba 图解(图 7-b)中, 样品点集中在富粘土区域, 综合分析, 扎杠流纹岩的源岩可能为地壳中的泥质岩夹杂砂岩;④有实验研究表明, $\text{Mg}^\#$ 值可用来示踪岩浆源区。 $\text{Mg}^\#<40$ 指示岩浆来源于下地壳, $\text{Mg}^\#>40$ 暗示岩浆可能为地幔来源(Rapp and Watson, 1995)。扎杠流纹岩的

$\text{Mg}^\#$ 值为 17.3~30.3, 平均为 24.1, 说明其可能来源于下地壳;⑤一般认为亏损地幔或新生壳源物质部分熔融形成的岩石 $\varepsilon_{\text{Hf}}(t)>0$, 而发生部分熔融的地壳物质形成的岩石 $\varepsilon_{\text{Hf}}(t)<0$ (Vervoort and Blichert-Toft, 1999; Griffina et al., 2004), 扎杠流纹岩的 $\varepsilon_{\text{Hf}}(t)$ 值变化范围较小, 介于 -2.0~5.5 之间, 平均为 -3.7, 均为负值, 指示其不可能是幔源岩浆与壳源岩浆混合的产物, 应为地壳部分熔融的产物(张博川, 2021);其 Hf 同位素二阶段模式年龄为 1581~1752 Ma, 表明源区可能为中元古代地壳物质。综合上述几点原因, 笔者认为扎杠流纹岩可能是由幔源岩浆加热下地壳物质使其部分熔融而形成。

通过对扎杠流纹岩主量、微量元素及锆石的地球化学特征进行综合分析, 笔者认为, 扎杠流纹

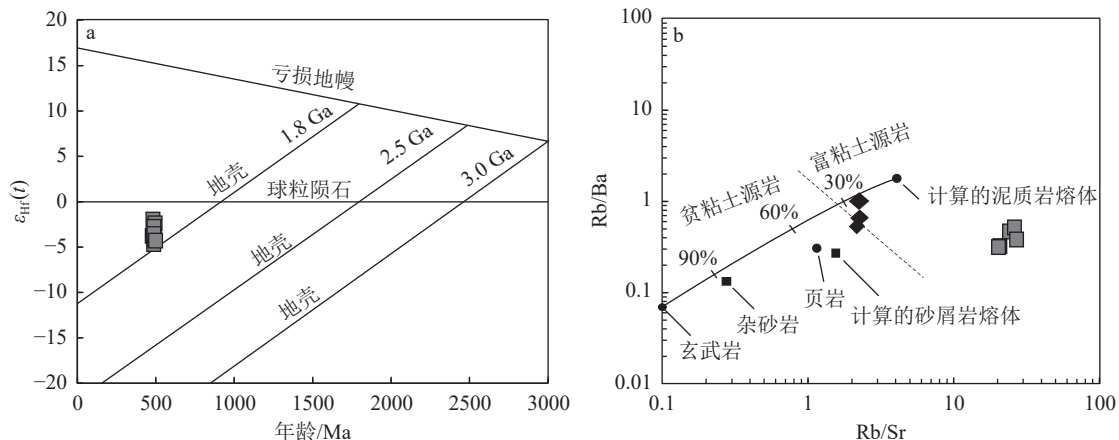


图7 扎扛流纹岩锆石年龄- $\epsilon_{\text{Hf}}(t)$ 图解(a)和Rb/Sr-Rb/Ba协变关系图解(b, 底图据Sylver, 1998)

Fig. 7 The zircon age- $\epsilon_{\text{Hf}}(t)$ diagram (a) and the Rb/Sr-Rb/Ba covariant relationship diagram (b) for the rhyolite from Zhakang

岩应该是幔源基性岩浆的加热导致下地壳物质部分熔融, 后期又发生结晶分异作用喷出地表形成的, 为高分异S型花岗岩。

4.3 构造意义及其对原特提斯洋俯冲的启示

4.3.1 对申扎地区扎扛不整合时限的约束

在冈瓦纳北缘的众多地区都识别出了寒武系和奥陶系之间的角度不整合, 拉萨地块、喜马拉雅地区、尼泊尔及印度均有该角度不整合的记录。这些角度不整合事件, 暗示早古生代有一期强烈的构造运动在冈瓦纳大陆北缘发生(胡培远等, 2021b)。北拉萨地块申扎地区奥陶系与寒武系之间的角度不整合是目前青藏高原中南部地区报道的时代依据及地层信息保存最充分的不整合, 上覆的下奥陶统扎扛组与下伏寒武系扎欠群以近90°的角度不整合相交(计文化等, 2009; 李才等, 2010; 张天羽, 2018), 这也是中国首次在拉萨地块报道的奥陶系与寒武系之间的不整合(张天羽, 2018)。然而, 申扎不整合的形成时代还没有得到很好的约束, 可靠的化石依据在该不整合的寒武纪扎欠群中并没有被发现, 但是该群内的火山岩夹层可以为其提供时代依据。计文化等(2009)报道了扎扛地区变流纹岩的锆石U-Pb年龄为501±2 Ma, Hu et al. (2013)报道的扎欠流纹岩形成时代为525~510 Ma, 扎扛流纹岩时代为510.4±4 Ma, 并发现一组稍老的年龄(544.4±7.3 Ma), 张天羽(2018)报道的扎欠群中最小的变质石英砂岩碎屑锆石年龄为519±7 Ma。下奥陶统扎扛组是目前申扎地区有确切化石依据的最低层位, 地层内的笔石化石暗示其地质时代为早奥陶世阿雷尼格期 *Tetragrap-*

*tus app rox imatus*带至 *Didymograp tus*(*Corymbograp tus*)*def lex us*带(程立人等, 2005)。综上所述, 张天羽(2018)提出晚寒武世晚期—早奥陶世早期可能为申扎地区扎扛不整合的形成时代。

本文报道的扎扛地区流纹岩的锆石U-Pb年龄为485±5 Ma, 属于晚寒武世—早奥陶世。因此, 进一步限定了申扎地区扎扛不整合的形成时代为早奥陶世早期。

4.3.2 对原特提斯洋沿环冈瓦纳大陆北缘新俯冲作用的启示

近年来, 学者在冈瓦纳大陆北缘的研究工作中获得了一系列的同时代年龄信息(表4)。综合不同地区的年龄资料, 可以看出冈瓦纳大陆北缘在早古生代有广泛的岩浆作用发生, 且呈带状分布, 至少从土耳其、尼泊尔、伊朗, 经过中国青藏高原南部, 一直延伸至滇西地区(胡培远等, 2021b)。

虽然获得了大量的早古生代岩浆岩年龄, 但这些岩石的构造背景及岩石成因还没有得到很好的约束(胡培远等, 2021b)。对于这些早古生代岩浆岩的成因, 仍存在多种不同的认识: ①这些岩浆事件属于泛非期—早古生代造山运动的结果(许志琴等, 2005; 李才等, 2010), 但有研究表明, 这些分布在冈瓦纳大陆北缘的岩浆岩, 其年龄相对于泛非事件晚30~50 Ma(Cawood et al., 2007; 张泽明等, 2008), 且泛非造山带的位置与这些岩浆岩的大地构造位置不符(解超明等, 2021), 指示其可能与泛非运动无关; ②有学者认为, 冈瓦纳大陆北缘处于活动大陆边缘环境, 这些岩浆岩可能是早古生代时期, 在冈瓦纳大陆北缘,

表 4 冈瓦纳大陆北缘早古生代岩浆岩年龄数据统计
Table 4 Summary of age data for the Early Paleozoic magmatic rocks along the northern margin of Gondwana Continent

构造位置	岩性	年龄/Ma	文献来源
北拉萨	变质流纹岩	525~510	Hu et al., 2013
北拉萨	流纹岩	501	计文化等, 2009
北拉萨	辉长岩	518、502	Hu et al., 2021
北拉萨	花岗岩	511~491	Hu et al., 2021
北拉萨	花岗岩	510	Gehrels et al., 2011
北拉萨	变质玄武岩	492	Zhu et al., 2012
北拉萨	变质流纹岩	492	Zhu et al., 2012
北拉萨	花岗片麻岩	531	Xu et al., 1985
北拉萨	花岗片麻岩	488	解超明等, 2010
北拉萨	花岗岩	532~482	Gwynn et al., 2012
北拉萨	花岗片麻岩	517~505	Xie et al., 2013
北拉萨	花岗片麻岩	502~487	Zhang et al., 2012
北拉萨	花岗片麻岩	510、505	贞晓瑞等, 2019
北拉萨	花岗岩	507	李才等, 2008
南羌塘	辉长岩和玄武岩	490~483	Liu et al., 2019a
南羌塘	花岗片麻岩	502~492	Liu et al., 2016
南羌塘	花岗岩	486、480	Hu et al., 2015
保山	玄武岩	499	杨学俊等, 2012
贡山	片麻状花岗岩	487	Song et al., 2007
贡山	花岗岩	473、461	刘琦胜等, 2012
腾冲	花岗岩	470	Chen et al., 2007
腾冲	片麻岩	489	林仕良等, 2012
喜马拉雅	玄武岩	496	Miller et al., 2001
喜马拉雅	花岗岩	475	Cawood et al., 2007
喜马拉雅	片麻岩	506、527	Quigley et al., 2008
喜马拉雅	片麻状花岗闪长岩	499	时超等, 2010
喜马拉雅	片麻岩	499	王晓先等, 2011
尼泊尔	花岗岩	473~484	Gehrels et al., 2003
伊朗	流纹岩	547~525	Ramezani et al., 2003
伊朗	花岗岩	549	Hassanzadeh et al., 2008
土耳其	花岗岩	531、546	Ustaömer et al., 2009

原特提斯洋洋壳发生俯冲导致的安第斯型岩浆活动(Cawood and Buchan, 2007; Cawood et al., 2007; Zhu et al., 2012; Zhang et al., 2014),且有研究表明,与原特提斯洋洋壳有关的早古生代岩浆作用分布在青藏高原南部(Hu et al., 2013, 2015; Ding et al., 2015;

Wang et al., 2020a, b; 解超明等, 2021);③另一些学者认为,泛非造山运动之后的后碰撞伸张拆离环境可以代表这些岩浆岩的形成环境(Liu et al., 2009; Li et al., 2016; 张天羽, 2018; Liu et al., 2019, 2020);④也有学者认为,冈瓦纳大陆北缘早古生代花岗岩是一个潜在的硅质大火成岩省的遗迹(Dan et al., 2022)。

笔者认为,扎杠地区晚寒武世—早奥陶世流纹岩是原特提斯洋沿环冈瓦纳大陆北缘新的俯冲作用导致的安第斯型岩浆活动的产物,主要有以下几点原因:①上文已经指出这些沿冈瓦纳北缘分布的早古生代岩浆与泛非运动无关;②前人研究表明,冈瓦纳大陆北缘的岩浆岩多为与俯冲作用相关的安第斯型岩浆(Liu et al., 2009; Zhu et al., 2012; Hu et al., 2013, 2015; Zhang et al., 2014; 胡培远等, 2021a, b),且在Yb-Ta 和 Rb/30-Hf-Ta×3 构造环境判别图解(图 8-a, b)中,扎杠流纹岩落入火山弧花岗岩区域,与前人报道的冈瓦纳大陆北缘岛弧岩浆岩具有相同的构造环境,而在 Yb-Th/Ta 图解(图 7-c)中,样品点落入活动大陆边缘及大洋岛弧区域,指示其形成于活动大陆边缘环境,且该流纹岩具有岛弧岩浆岩的特征(Rb、Th、Pb 等元素富集, Nb、Ta、Ti 等高场强元素亏损; 雷聪聪等, 2024);③申扎地区寒武系与奥陶系近 90°的角度不整合(李才等, 2010)也指示其并非形成于拉张背景下;④Cawood et al.(2007)认为,冈瓦纳超大陆的最终拼合于约 510 Ma 完成,并导致冈瓦纳原特提斯边缘的俯冲带开始,相关的安第斯型岩浆活动在 530~470 Ma 活跃,本文的流纹岩形成时代(485 Ma)在这个时期内,可能是冈瓦纳北缘安第斯型岩浆的一部分。

研究表明,在洋壳经历低角度俯冲时,沉积岩能够随之被深埋,然后由低角度向高角度变换,沉积岩发生部分熔融,形成 S 型花岗岩的原始岩浆(Collins and Richards, 2008; 张洪亮等, 2019)。综合上述分析,笔者认为,扎杠流纹岩应为早古生代原特提斯洋洋壳向冈瓦纳大陆北缘低角度俯冲时,导致下地壳沉积物埋深后又向高角度转换引起的部分熔融而形成的 S 型花岗岩,为早古生代冈瓦纳大陆北缘安第斯型岩浆活动的一部分。

5 结 论

(1)拉萨地块申扎地区流纹岩的 LA-ICP-MS

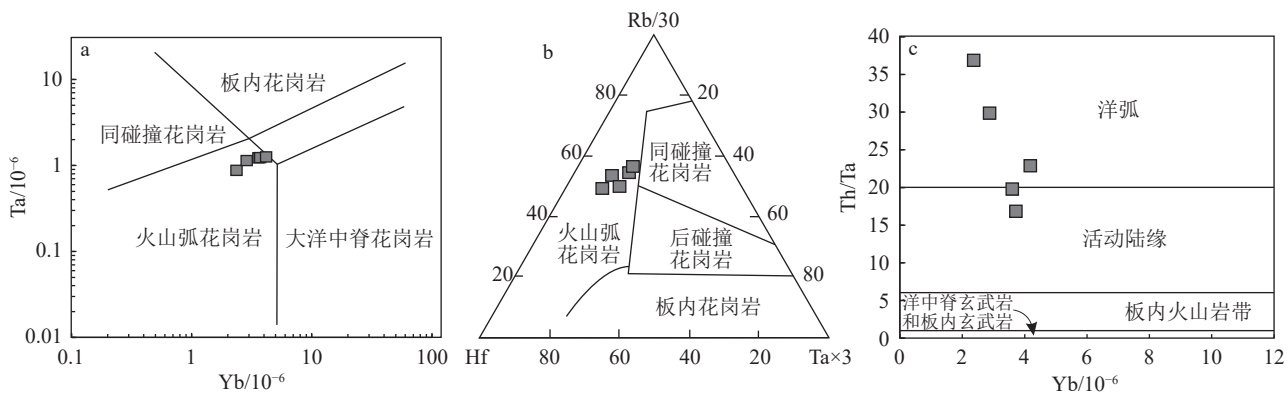


图8 申扎地区早奥陶世流纹岩 Yb-Ta(a, 底图据支倩等, 2023)、Rb/30-Hf-Tax3(b, 底图据胡培远等, 2021b)和 Yb-Th/Ta(c, 底图据 Gorton and Schandl, 2000)构造环境判别图解

Fig. 8 Yb-Ta(a), Rb/30-Hf-Tax3(b) and Yb-Th/Ta(c) tectonic setting discrimination diagrams of the Early Ordovician rhyolite from Xainza

锆石 $^{206}\text{Pb}/^{238}\text{U}$ 年龄加权平均值为 485 ± 5 Ma, 为晚寒武世—早奥陶世, 进一步限定了申扎地区奥陶纪与寒武系不整合的形成时间应在早奥陶世早期。

(2) 扎扛流纹岩分异指数较高, 可能经历了强烈的结晶分异作用, 具有类似高分异S型花岗岩的特征, 其源区可能为下地壳的沉积物, 具有岛弧岩浆岩的地球化学特征。

(3) 扎扛流纹岩是原特提斯洋洋壳向冈瓦纳大陆北缘低角度俯冲时导致下地壳沉积物埋深后又向高角度转换引起的部分熔融而形成的S型花岗岩, 为早古生代冈瓦纳大陆北缘安第斯型岩浆活动的一部分。

致谢:衷心地感谢吉林大学地球科学学院王斌和宋宇航博士在野外采样工作中给予的帮助, 感谢审稿人对本文提出的宝贵修改意见。

References

- Allégre C J, Courtillot V, Tapponnier P, et al. 1984. Structure and evolution of the Himalaya–Tibet orogenic belt[J]. *Nature*, 307(5946): 17–22.
- Cawood P A, Buchan C. 2007. Linking accretionary orogenesis with supercontinent assembly[J]. *Earth–Science Reviews*, 82(3): 217–256.
- Cawood P A, Johnson M R W, Nemchin A A. 2007. Early Palaeozoic orogenesis along the Indian margin of Gondwana: Tectonic response to Gondwana assembly[J]. *Earth and Planetary Science Letters*, 255(1): 70–84.
- Chen F K, Li X H, Wang X L, et al. 2007. Zircon age and Nd–Hf isotopic composition of the Yunnan Tethyan belt, southwestern China[J]. *International Journal of Earth Sciences*, 96(6): 1179–1194.
- Chen J L, Zhao W X, Xu J F, et al. 2012. Geochemistry of Miocene trachytes in Bugasi, Lhasa block, Tibetan Plateau: Mixing products between mantle-and crust-derived melts? [J]. *Gondwana Research*, 21: 112–122.
- Chen S Y, Yang J S, Li Y, et al. 2009. Ultramafic blocks in Sumdo region, Lhasa block, Eastern Tibet plateau: An ophiolite unit[J]. *Journal of Earth Science*, 20(2): 332–347.
- Cheng L R, Zhang Y C, Zhang Y J. 2005. Discovery of the early Ordovician strata in Xianza county, Tibet and its significance[J]. *Journal of Stratigraphy*, (1): 38–41(in Chinese with English abstract).
- Civetta L, D’Antonio M, Orsi G, et al. 1998. The geochemistry of volcanic rocks from Pantelleria Island, Sicily Channel: petrogenesis and characteristics of the mantle source region[J]. *Journal of Petrology*, 39(8): 1453–1491.
- Clemens J. 2003. S-type granitic magmas—petrogenetic issues, models and evidence[J]. *Earth–Science Reviews*, 61(1/2): 1–18.
- Collins A S, Pisarevsky S A. 2005. Amalgamating eastern Gondwana: The evolution of the Circum–Indian Orogens[J]. *Earth–Science Reviews*, 71(3): 229–270.
- Collins W J, Richards S W. 2008. Geodynamic significance of S-type granites in circum–Pacific orogens[J]. *Geology*, 36(7): 559–562.
- Collins W J. 1982. Nature and Origin of a Type Granites with Particular Reference to Southeastern Australia[J]. *Contribution to Mineralogy and Petrology*, 80(2): 189–200.
- Dan W, Murphy J B, Tang G J, et al. 2022. Cambrian–Ordovician magmatic flare-up in NE Gondwana: A silicic large igneous province? [J]. *GSA Bulletin*, 135(5/6): 1618–1632.
- Ding H X, Zhang Z M, Dong X, et al. 2015. Cambrian ultrapotassic rhyolites from the Lhasa terrane, south Tibet: Evidence for Andean-type magmatism along the northern active margin of Gondwana[J]. *Gondwana Research*, 27(4): 1616–1629.
- Ding H X. 2015. The Petrogenesis and tectonic significance of the early Paleozoic and late Mesozoic volcanics from the Lhasa terrane, south Tibet[D]. A Dissertation for Doctor Degree Submitted to Chinese Academy of Geological Science: 1–131 (in Chinese with English)

- abstract).
- Dong X, Zhang Z M, Wang J L, et al. 2009. Provenance and formation age of the Nyingchi Group in the southern Lhasa terrane, Tibetan Plateau: Petrology and zircon U-Pb geochronology[J]. *Acta Petrologica Sinica*, 25(7): 1678–1694(in Chinese with English abstract).
- Dong Y C. 2021. The metamorphism of Sumdo High/Ultra High pressure in Tibet and its tectonic significance[D]. PhD Dissertation of Jilin University: 1–137(in Chinese with English abstract).
- Duan M L, Xie C M, Wang B, et al. 2022. Ocean Island Rock Assembly and Its Tectonic Significance in Tangga–Sumdo Area, Tibet[J]. *Earth Science*, 47(8): 2968–2984(in Chinese with English abstract).
- Fan J J, Li C, Wang M, et al. 2018. Material composition, age and significance of the Dong Co Melange in the Bangong Co–Nujiang suture zone[J]. *Geological Bulletin of China*, 37(8): 1417–1427(in Chinese with English abstract).
- Gehrels G E, DeCelles P G, Martin A, et al. 2003. Initiation of the Himalayan orogen as an early Paleozoic thin-skinned thrust belt[J]. *GSA Today*, 13(9): 4–9.
- Gehrels G E, DeCelles P G, Ojha T P, et al. 2006. Geologic and U–Th–Pb geochronologic evidence for early Paleozoic tectonism in the Kathmandu thrust sheet, central Nepal Himalaya[J]. *Geological Society of America Bulletin*, 118(1/2): 185–198.
- Gehrels G, Kapp P, DeCelles P, et al. 2011. Detrital zircon geochronology of pre-Tertiary strata in the Tibetan–Himalayan orogen[J]. *Tectonics*, 30(5): 2011TC002868.
- Gorton M P, Schandl E S. 2000. From continents to island arcs: a geochemical index of tectonic setting for arc-related and within-plate felsic to intermediate volcanic rocks[J]. *The Canadian Mineralogist*, 38: 1065–1073.
- Griffina W L, Belousova E A, Shee S R, et al. 2004. Archean crustal evolution in the northern Yilgarn Craton: U–Pb and Hf-isotope evidence from detrital zircons[J]. *Precambrian Research*, 131(3/4): 231–282.
- Grimes C B, John B E, Kelemen P B, et al. 2007. Trace element chemistry of zircons from oceanic crust: a method for distinguishing detrital zircon provenance[J]. *Geology*, 35: 643–646.
- Guynn J, Kapp P, Gehrels G E, et al. 2012. U–Pb geochronology of basement rocks in central Tibet and paleogeographic implications[J]. *Journal of Asian Earth Sciences*, 43(1): 23–50.
- Harris N B W, Inger S. 1992. Trace element modelling of pelite-derived granites[J]. *Contributions to Mineralogy and Petrology*, 110(1): 46–56.
- Harris N B W, Pearce J A, Tindle A G. 1986. Geochemical characteristics of collision-zone magmatism[J]. Geological Society, London, Special Publications, 19: 67–81.
- Hassanzadeh J, Stockli D F, Horton B K, et al. 2008. U–Pb zircon geochronology of late Neoproterozoic–Early Cambrian granitoids in Iran: Implications for paleogeography, magmatism, and exhumation history of Iranian basement[J]. *Tectonophysics*, 451(1): 71–96.
- Hastie A R, Kerr A C, Pearce J A, et al. 2007. Classification of altered volcanic island arc rocks using immobile trace elements: Development of the Th–Co discrimination diagram[J]. *Journal of Petrology*, 48: 2341–2357.
- Hu P Y, Li C, Wang M, et al. 2013. Cambrian volcanism in the Lhasa terrane, southern Tibet: Record of an early Paleozoic Andean-type magmatic arc along the Gondwana proto-Tethyan margin[J]. *Journal of Asian Earth Sciences*, 77: 91–107.
- Hu P Y, Zhai Q G, Cawood P A, et al. 2021. Cambrian magmatic flare-up, central Tibet: Magma mixing in proto-Tethyan arc along north Gondwanan margin[J]. *GSA Bulletin*, 133(9/10): 2171–2188.
- Hu P Y, Zhai Q G, Jahn B M, et al. 2015. Early Ordovician granites from the South Qiangtang terrane, northern Tibet: Implications for the early Paleozoic tectonic evolution along the Gondwanan proto-Tethyan margin[J]. *Lithos*, 220/223: 318–338.
- Hu P Y, Zhai Q G, Tang Y, et al. 2021b. Geochemistry, zircon U–Pb age, Lu–Hf isotopes and tectonic setting of the Early Paleozoic gneissic granites from the Nyainrong microcontinent, Tibet Plateau[J]. *Geological Bulletin of China*, 40(8): 1203–1214(in Chinese with English abstract).
- Hu P Y, Zhai Q G, Zhao G C, et al. 2019. Late Cryogenian magmatic activity in the North Lhasa terrane, Tibet: Implication of slab break-off process[J]. *Gondwana Research*, 71: 129–149.
- Hu P Y, Zhai Q G, Zhao G C, et al. 2021a. Andean-type orogeny along the northern Gondwana margin: Evidences of zircon U–Pb ages and geochemistry data of the Ordovician granites from the Amdo area, northern Tibet[J]. *Acta Petrologica Sinica*, 37(2): 530–544(in Chinese with English abstract).
- Hu Z C, Liu Y S, Gao S, et al. 2012. Improved in situ Hf isotope ratio analysis of zircon using newly designed X skimmer cone and jet sample cone in combination with the addition of nitrogen by laser ablation multiple collector ICP-MS[J]. *Journal of Analytical Atomic Spectrometry*, 27(9): 1391–1399.
- Ji W H, Chen S J, Zhao Z M, et al. 2009. Discovery of the Cambrian volcanic rocks in the Xainza area Gangdese orogenic belt, Tibet, China and its significance[J]. *Geological Bulletin of China*, 28(9): 1350–1354(in Chinese with English abstract).
- Jung S, Pfander J A. 2007. Source composition and melting temperatures of orogenic granitoids from CaO/Na₂O, Al₂O₃/TiO₂ and accessory mineral saturation thermometry[J]. *European Journal of Mineralogy*, 19(6): 859–870.
- Kemp A I S, Hawkesworth C J, Foster G L, et al. 2006. Magmatic and Crustal Differentiation History of Granitic Rocks from Hf–O Isotopes in Zircon[J]. *Science*, 315(5814): 980–983.
- Kemp A I S, Hawkesworth C J, Paterson B A, et al. 2008. Exploring the plutonic–volcanic link: A zircon U–Pb, Lu–Hf and O isotope study of paired volcanic and granitic units from southeastern Australia[J]. *Earth and Environmental Science Transactions of The Royal Society of Edinburgh*, 97(4): 337–355.
- Lee C T, Morton D M. 2015. High silica granites: Terminal porosity and crystal setting in shallow magma chambers[J]. *Earth & Planetary Science Letters*, 409(409): 23–31.

- Lei C C, Ma J, Bo H J, et al. 2024. The zircon U–Pb geochronology, geochemistry and tectonic environment of the Weibozhan intermediate–felsic rocks in the northern margin of the Alxa block[J]. *Geological Bulletin of China*, DOI:10.12097/j.issn.2022.03.026.
- Li C, Wu Y W, Wang M, et al. 2010. Significant progress on Pan African and Early Paleozoic orogenic events in Qinghai-Tibet Plateau discovery of Pan-African orogenic unconformity and Cambrian System in the Gangdise area, Tibet, China[J]. *Geological Bulletin of China*, 29(12): 1733–1736(in Chinese with English abstract).
- Li C, Xie Y W, Sha S L, et al. 2008. SHRIMP U–Pb zircon dating of the Pan-African granite in Baxoi County, eastern Tibet, China[J]. *Geological Bulletin of China*, 27(1): 64–68(in Chinese with English abstract).
- Li C. 2008. A review on 20 years' study of the Longmu Co-Shuanghu–Lancang River Suture Zone in Qinghai-Xizang (Tibet) Plateau[J]. *Geological Review*, 54(1): 105–119(in Chinese with English abstract).
- Li G J, Wang Q F, Huang Y H, et al. 2016. Petrogenesis of middle Ordovician peraluminous granites in the Baoshan block: Implications for the early Paleozoic tectonic evolution along East Gondwana[J]. *Lithos*, 245: 76–92.
- Li W F, Pan T, Wang B Z, et al. 2022. Ordovician magmatic arc in the Nanshan area, Qinghai Province: Evidence from zircon U–Pb chronology, element geochemistry and Hf isotope compositions of the diorites in the Chakaibeishan area[J]. *Geotectonica et Metallogenica*, 46(4): 788–802(in Chinese with English abstract).
- Lin S L, Cong F, Gao Y J, et al. 2012. LA –ICP –MS zircon U –Pb age of gneiss from Gaoligong Mountain Group on the southeastern margin of Tengchong block in western Yunnan Province[J]. *Geological Bulletin of China*, 31(2/3): 258–263(in Chinese with English abstract).
- Linnen R L, Keppler H. 2002. Melt composition control of Zr/Hf fractionation in magmatic processes[J]. *Geochimica et Cosmochimica Acta*, 66(18): 3293–3301.
- Liu C Z, Chung S L, Wu F Y, et al. 2016. Tethyan suturing in Southeast Asia: Zircon U–Pb and Hf–O isotopic constraints from Myanmar ophiolites[J]. *Geology*, 44(4): 311–314.
- Liu D, Zhao Z D, Zhu D C, et al. 2011. The petrogenesis of postcollisional potassic–ultrapotassic rocks in Xungba basin, western Lhasa terrane: Constraints from zircon U–Pb geochronology and geochemistry[J]. *Acta Petrologica Sinica*, 27(7): 2045–2059(in Chinese with English abstract).
- Liu Q S, Ye P S, Wu Z H. 2012. SHRIMP zircon U–Pb dating and petrogeochemistry of Ordovician granite bodies in the southern segment of Gaoligong Mountain, western Yunnan Province[J]. *Geological Bulletin of China*, 31(2/3): 250–257(in Chinese with English abstract).
- Liu S, Hu R Z, Gao S, et al. 2009. U–Pb zircon, geochemical and Sr–Nd–Hf isotopic constraints on the age and origin of Early Palaeozoic I-type granite from the Tengchong–Baoshan Block, Western Yunnan Province, SW China[J]. *Journal of Asian Earth Sciences*, 36(2): 168–182.
- Liu Y M, Li C, Wang M, et al. 2014. Geochemical characteristics of Wanghuling Formation rhyolite in the Qiangtang Basin and their geological significance[J]. *Geological Bulletin of China*, 33(11): 1759–1767(in Chinese with English abstract).
- Liu Y M, Li C, Xie C M, et al. 2016. Cambrian granitic gneiss within the central Qiangtang terrane, Tibetan Plateau: implications for the early Palaeozoic tectonic evolution of the Gondwanan margin[J]. *International Geology Review*, 58(9): 1043–1063.
- Liu Y M, Li S Z, Santosh M, et al. 2019. The generation and reworking of continental crust during early Paleozoic in Gondwanan affinity terranes from the Tibet Plateau[J]. *Earth–Science Reviews*, 190: 486–497.
- Liu Y M, Li S Z, Santosh M, et al. 2020. The passive margin of northern Gondwana during Early Paleozoic: Evidence from the central Tibet Plateau[J]. *Gondwana Research*, 78: 126–140.
- Liu Y M, Xie C M, Li C, et al. 2019. Breakup of the northern margin of Gondwana through lithospheric delamination: Evidence from the Tibetan Plateau[J]. *GSA Bulletin*, 131(3/4): 675–697.
- Liu Y S, Gao S, Hu Z C, et al. 2010. Continental and oceanic crust recycling-induced melt–peridotite interactions in the Trans–North China Orogen: U–Pb dating, Hf isotopes and trace elements in zircons from mantle xenoliths[J]. *Journal of Petrology*, 51(1/2): 537–571.
- Liu Z Q. 2006. Permo–Carboniferous clastic sediments of the Yongzhu area, Xainza, Tibet and their possible sedimentary environments[D]. A Dissertation for Master Degree Submitted to Chinese Academy of Geological Science: 1–62(in Chinese with English abstract).
- Luo A B. 2022. Timing and process of the extinction of the Bangong–Nujiang Ocean: Insights from Early Cretaceous sedimentary and volcanic rocks[D]. A Dissertation for Doctor Degree Submitted to Jilin University: 1–232(in Chinese with English abstract).
- Lustrino M, Melluso L, Morra V. 2000. The role of lower continental crust and lithospheric mantle in the genesis of Plio–Pleistocene volcanic rocks from Sardinia (Italy)[J]. *Earth and Planetary Science Letters*, 180(3/4): 259–270.
- Maniar P D, Piccoli P M. 1989. Tectonic discrimination of granitoids[J]. *Geological Society of America Bulletin*, 101(5): 635–643.
- Meert J G. 2003. A synopsis of events related to the assembly of eastern Gondwana[J]. *Tectonophysics*, 362(1): 1–40.
- Miller C, Thöni M, Frank W, et al. 2001. The early Palaeozoic magmatic event in the Northwest Himalaya, India: source, tectonic setting and age of emplacement[J]. *Geological Magazine*, 138(3): 237–251.
- Murphy J B, van Staal C R, Collins W J. 2011. A comparison of the evolution of arc complexes in Paleozoic interior and peripheral orogens: Speculations on geodynamic correlations[J]. *Gondwana Research*, 19(3): 812–827.
- Pan G T, Wang L Q, Li R S, et al. 2012. Tectonic evolution of the Qinghai–Tibet Plateau[J]. *Journal of Asian Earth Sciences*, 53: 3–14.
- Pearce J A, Harris N B W, Tindle A G. 1984. Trace element discrimination diagrams for the tectonic interpretation of granitic rocks[J]. *Petrol*, 25: 956–983.
- Pearce J A. 1983. Trole of sub-continental lithosphere in magma genesis at destructive plate margins[C]//Hawkesworth C J, Norry M J.

- Continental Basalts and Mantle Xenoliths. Nantwich Shiva: Academic Press: 230–249.
- Peccerillo A, Taylor S R. 1976. Geochemistry of eocene calc-alkaline volcanic rocks from the Kastamonu area, Northern Turkey[J]. *Contributions to Mineralogy and Petrology*, 58(1): 63–81.
- Quigley M C, Liangjun Y, Gregory C, et al. 2008. U-Pb SHRIMP zircon geochronology and T-t-d history of the Kampa Dome, southern Tibet[J]. *Tectonophysics*, 446(1): 97–113.
- Ramezani J. 2003. The Saghand Region, Central Iran: U-Pb geochronology, petrogenesis and implications for Gondwana Tectonics[J]. *American Journal of Science*, 303(7): 622–665.
- Rapp R P, Watson E B. 1995. Dehydration melting of metabasalt at 8~32kbar: Implications for continental growth and crust-mantle recycling[J]. *Journal of Petrology*, 36(4): 891–931.
- Ronga F, Lustrino M, Marzoli A, et al. 2010. Petrogenesis of a basalt-comendite-pantellerite rock suite: the Boseti Volcanic Complex (Main Ethiopian Rift)[J]. *Mineralogy and Petrology*, 98(1/4): 227–243.
- Shi C, Li R S, He S P, et al. 2010. LA-ICP-MS zircon U-Pb dating for gneissic garnet-bearing biotite granodiorite in the Yadong area, southern Tibet, China and its geological significance[J]. *Geological Bulletin of China*, 29(12): 1745–1753(in Chinese with English abstract).
- Song S G, Ji J Q, Wei C J, et al. 2007. Early Paleozoic granite in Nujiang River of northwest Yunnan in southwestern China and its tectonic implications[J]. *Chinese Science Bulletin*, 52(17): 2402–2406.
- Sun S S, McDonough W F. 1989. Chemical and isotopic systematics of oceanic basalts: implications for mantle composition and processes[J]. Geological Society, London, Special Publications, 42(1): 313–345.
- Sylver P J. 1998. Post-collisional strongly peraluminous granites[J]. *Lithos*, 45: 29–44.
- Tischendorf G, Paelchen W. 1985. Zur Klassifikation von Granitoiden/Classification of Granitoids[J]. *Zeitschrift fuer Geologische Wissenschaften*, 13(5): 615–627.
- Ustaömer P A, Ustaömer T, Collins A S, et al. 2009. Cadomian (Ediacaran-Cambrian) arc magmatism in the Bitlis Massif, SE Turkey: Magmatism along the developing northern margin of Gondwana[J]. *Tectonophysics*, 473(1): 99–112.
- Vervoort J D, Blichert-Toft J. 1999. Evolution of the depleted mantle: Hf isotope evidence from juvenile rocks through time[J]. *Geochemica et Cosmochimica Acta*, 63: 533–566.
- Wang B D, Wang L Q, Wang, D B, et al. 2018. Tectonic Evolution of the Changning-Menglian Proto-Paleo Tethys Ocean in the Sanjiang Area, Southwestern China[J]. *Earth Science*, 43(8): 2527–2550(in Chinese with English abstract).
- Wang H T, Zhai Q G, Hu P Y, et al. 2020a. Early Paleozoic granitic rocks of the South Qiangtang Terrane, northern Tibetan Plateau: Implications for subduction of the Proto-(Paleo-) Tethys Ocean[J]. *Journal of Asian Earth Sciences*, 204: 104579.
- Wang H T, Zhai Q G, Hu P Y, et al. 2020b. Late Cambrian to Early Silurian Granitic Rocks of the Gemuri Area, Central Qiangtang, North Tibet: New Constraints on the Tectonic Evolution of the Northern Margin of Gondwana[J]. *Acta Geologica Sinica*, 94(4): 1007–1019.
- Wang Q, Zhao Z H, Xiong X L. 2000. The Ascertainment of Late-Yanshanian A-type Granite in Tongbai-Dabie Orogenic Belt[J]. *Acta Petrologica Mineralogica*, 19(4): 297–306(in Chinese with English abstract).
- Wang X X, Zhang J J, Yang X Y, et al. 2011. Zircon SHRIMP U-Pb ages, Hf isotopic features and their geological significance of the Greater Himalayan crystalline complex augen gneiss in Gyirong area, south Tibet[J]. *Earth Science Frontiers*, 18(2): 127–139(in Chinese with English abstract).
- Watson E B, Harrison T M. 1983. Zircon saturation revisited—temperature and composition effects in a variety of crustal magma types[J]. *Earth and Planetary Science Letters*, 64(2): 295–304.
- Wedepohl K H. 1995. The composition of the continental crust[J]. *Geochimica et cosmochimica Acta*, 59(7): 1217–1232.
- Whalen J B, Currie K L, Chappell B W. 1987. A-type granites: Geochemical characteristics, discrimination and pretrogenesis[J]. *Contrib Mineral Petrol*, 95(4): 407–419.
- Wilson M. 1989. Igneous Petrology: A Global Tectonic Approach[M]. London: Unwin Hyman: 1–466.
- Winchester J A, Floyd P A. 1977. Geochemical discrimination of different magmas and their differentiation products using immobile elements[J]. *Chemical Geology*, 20: 325–343.
- Wu F Y, Li X H, Yang J H, et al. 2007. Discussions on the petrogenesis of granites[J]. *Acta Petrologica Sinica*, 23(6): 1217–1238(in Chinese with English abstract).
- Wu F Y, Liu C Z, Zhang L L, et al. 2014. Yarlung Zangbo ophiolite: A critical updated view[J]. *Acta Petrologica Sinica*, 30(2): 293–325(in Chinese with English abstract).
- Wu H, Zhai Q G, Hu P Y, et al. 2021. Early Cretaceous volcanic rocks in northern Baingoin, Tibet: Magmatic record of the closure of the Bangong-Nujiang Ocean[J]. *Geology in China*, 48(5): 1623–1638(in Chinese with English abstract).
- Xie C M, Duan M L, Yu Y P, et al. 2019. Genesis and geological significance of Early Jurassic metamorphic gabbro in the Sumdo area, Tibet[J]. *Acta Petrologica Sinica*, 35(10): 3065–3082(in Chinese with English abstract).
- Xie C M, Li C, Su L, et al. 2010. LA-ICP-MS U-Pb dating of zircon from granite-gneiss in the Amdo area, northern Tibet, China[J]. *Geological Bulletin of China*, 29(12): 1737–1744(in Chinese with English abstract).
- Xie C M, Li C, Su L, et al. 2013. Pan-African and early Paleozoic tectonothermal events in the Nyainrong microcontinent: Constraints from geochronology and geochemistry[J]. *Science China Earth Sciences*, 56(12): 2066–2079.
- Xie C M, Li C, Wang M, et al. 2014. Tectonic affinity of the Nyainrong microcontinent: Constraints from zircon U-Pb age and Hf isotopes compositions[J]. *Geological Bulletin of China*, 33(11): 1778–1792(in Chinese with English abstract).
- Xie C M, Li C, Zhai Q G, et al. 2021. The Early Paleozoic magmatism in

- Qiangtang, northern Tibet and its geological significance[J]. *Sedimentary Geology and Tethyan Geology*, 41(2): 340–350(in Chinese with English abstract).
- Xu R H, Schärer U, Allègre C J. 1985. Magmatism and metamorphism in the Lhasa Block (Tibet): A geochronological study[J]. *The Journal of Geology*, 93(1): 41–57.
- Xu W T, Zhang X H, Zhang B B, et al. 2022. Genesis of highly fractionated S-type granites: Evidence from zircon U-Pb age, Hf isotopes and geochemistry of Fuguanshan pluton, Northeastern Jiangxi Province[J]. *Geological Bulletin of China*, 41(4): 577–589(in Chinese with English abstract).
- Xu Z Q, Dilek Y, Cao H, et al. 2015. Paleo-Tethyan evolution of Tibet as recorded in the East Cimmerides and West Cathaysides[J]. *Journal of Asian Earth Sciences*, 105: 320–337.
- Xu Z Q, Yang J S, Liang F H, et al. 2005. Pan-African and Early Paleozoic orogenic events in the Himalaya terrane: Inference from SHRIMP U-Pb zircon ages[J]. *Acta Petrologica Sinica*, 21(1): 1–12(in Chinese with English abstract).
- Yang J S, Xu Z Q, Li Z L, et al. 2009. Discovery of an eclogite belt in the Lhasa block, Tibet: A new border for Paleo-Tethys?[J]. *Journal of Asian Earth Sciences*, 34(1): 76–89.
- Yang X J, Jia X C, Xiong C L, et al. 2012. LA-ICP-MS zircon U-Pb age of metamorphic basic volcanic rock in Gongyanghe Group of southern Gaoligong Mountain, western Yunnan Province, and its geological significance[J]. *Geological Bulletin of China*, 31(2/3): 264–276(in Chinese with English abstract).
- Yun X R, Cai Z H, He B Z, et al. 2019. Early Paleozoic and Mesozoic orogenic records in Amdo region, Tibet: Zircon U-Pb geochronology and Hf isotopic compositions from the Amdo micro-continent and South Qiangtang terrane[J]. *Acta Petrologica Sinica*, 35(6): 1673–1692(in Chinese with English abstract).
- Zhang B C. 2021. Petrogenesis and Geological significance of Eocene rhyolites in the Wuma area, Tibet[D]. Master Dissertation of Jilin University: 1–51(in Chinese with English abstract).
- Zhang H L, Yang W G, Zhu L D, et al. 2019. Zircon U-Pb age, geochemical characteristics and geological significance of highly differentiated S-type granites in the south Lhasa block[J]. *Mineral Petrol*, 39(1): 52–62(in Chinese with English abstract).
- Zhang L L, Zhu D C, Zhao Z D, et al. 2011. Petrogenesis of magmatism in the Baerda region of Northern Gangdese Tibet: Constraints from geochemistry, geochronology and Sr-Nd-Hf isotopes[J]. *Acta Petrologica Sinica*, 26(6): 1871–1888 (in Chinese with English abstract).
- Zhang T Y. 2018. Early Paleozoic tectonic movement on the Tibetan Plateau and its adjacent areas: A case study of Cambrian-Ordovician unconformity[D]. Master Dissertation of Jilin University: 1–133(in Chinese with English abstract).
- Zhang Y X, Xie C M, Yu Y P, et al. 2018. The Early Jurassic subduction of Neo-Tethyan oceanic slab: Constraints from zircon U-Pb age and Hf isotopic compositions of Sumdo high-Mg diorite[J]. *Geological Bulletin of China*, 37(8): 1387–1399(in Chinese with English abstract).
- Zhang Z M, Dong X, Liu F, et al. 2012. Tectonic evolution of the Amdo Terrane, Central Tibet: Petrochemistry and zircon U-Pb geochronology[J]. *The Journal of Geology*, 120(4): 431–451.
- Zhang Z M, Dong X, Santosh M, et al. 2014. Metamorphism and tectonic evolution of the Lhasa terrane, Central Tibet[J]. *Gondwana Research*, 25(1): 170–189.
- Zhang Z M, Wang J L, Shen K, et al. 2008. Paleozoic circum-Gondwana orogens: Petrology and geochronology of the Namche Barwa Complex in the eastern Himalayan syntaxis, Tibet[J]. *Acta Petrologica Sinica*, 24(7): 1627–1637(in Chinese with English abstract).
- Zhi Q, Ren R, Duan F H, et al. 2023. Genetic mechanism of Late Carboniferous intermediate-acid volcanic rocks in southern West Junggar and its constraints on the closure of the Junggar Ocean[J]. *Earth Science Frontiers*, 31(3): 1–21 (in Chinese with English abstract).
- Zhu D C, Li S M, Cawood P A, et al. 2016. Assembly of the Lhasa and Qiangtang terranes in central Tibet by divergent double subduction[J]. *Lithos*, 245: 7–17.
- Zhu D C, Mo X X, Niu Y L, et al. 2009. Zircon U-Pb dating and in-situ Hf isotopic analysis of Permian peraluminous granite in the Lhasa terrane, southern Tibet: Implications for Permian collisional orogeny and paleogeography[J]. *Tectonophysics*, 469(1): 48–60.
- Zhu D C, Zhao Z D, Niu Y L, et al. 2011. The Lhasa Terrane: Record of a microcontinent and its histories of drift and growth[J]. *Earth and Planetary Science Letters*, 301(1): 241–255.
- Zhu D C, Zhao Z D, Niu Y L, et al. 2012. Cambrian bimodal volcanism in the Lhasa Terrane, southern Tibet: Record of an early Paleozoic Andean-type magmatic arc in the Australian proto-Tethyan margin[J]. *Chemical Geology*, 328: 290–308.
- Zhu D C, Zhao Z D, Niu Y L, et al. 2013. The origin and pre-Cenozoic evolution of the Tibetan Plateau[J]. *Gondwana Research*, 23(4): 1429–1454.

附中文参考文献

- 程立人, 张以春, 张予杰. 2005. 藏北申扎地区早奥陶世地层的发现及意义[J]. *地层学杂志*, (1): 38–41.
- 丁慧霞. 2015. 青藏高原拉萨地体北部早古生代与晚中生代火山岩的成因及构造意义[D]. 中国地质科学院博士学位论文: 1–131.
- 段梦龙, 解超明, 王斌, 等. 2022. 西藏唐加地区石炭纪洋岛型岩石组合及其构造意义[J]. *地球科学*, 47(8): 2968–2984.
- 董昕, 张泽明, 王金丽, 等. 2009. 青藏高原拉萨地体南部林芝岩群的物质来源与形成年代: 岩石学与锆石U-Pb年代学[J]. *岩石学报*, 25(7): 1678–1694.
- 董宇超. 2021. 西藏松多高压/超高压变质作用及其构造意义[D]. 吉林大学博士学位论文: 1–137.
- 范建军, 李才, 王明, 等. 2018. 班公湖-怒江缝合带洞错混杂岩物质组成、时代及其意义[J]. *地质通报*, 37(8): 1417–1427.
- 胡培远, 翟庆国, 唐跃, 等. 2021b. 青藏高原聂荣微陆块早古生代片麻状花岗岩地球化学、锆石U-Pb年龄和Lu-Hf同位素特征及构造背景[J]. *地质通报*, 40(8): 1203–1214.
- 胡培远, 翟庆国, 赵国春, 等. 2021a. 冈瓦纳大陆北缘安第斯型造山带:

- 藏北安多奥陶纪花岗岩锆石 U-Pb 年龄和地球化学证据 [J]. 岩石学报, 37(2): 530–544.
- 计文化, 陈守建, 赵振明, 等. 2009. 西藏冈底斯构造带申扎一带寒武系火山岩的发现及其地质意义 [J]. 地质通报, 28(9): 1350–1354.
- 雷聪聪, 马军, 薄海军, 等. 2024. 阿拉善地块北缘微波站中—酸性岩体锆石 U-Pb 年代学、岩石地球化学及构造环境 [J]. 地质通报, DOI:10.12097/j.issn.2022.03.026.
- 李才, 吴彦旺, 王明, 等. 2010. 青藏高原泛非—早古生代造山事件研究重大进展——冈底斯地区寒武系和泛非造山不整合的发现 [J]. 地质通报, 29(12): 1733–1736.
- 李才, 谢尧武, 沙绍礼, 等. 2008. 藏东八宿地区泛非期花岗岩锆石 SHRIMP U-Pb 定年 [J]. 地质通报, (1): 64–68.
- 李才. 2008. 青藏高原龙木错—双湖—澜沧江板块缝合带研究二十年 [J]. 地质论评, 54(1): 105–119.
- 李献华, 李武显, 李正祥. 2007. 再论南岭燕山早期花岗岩的成因类型与构造意义 [J]. 科学通报, 52(9): 981–991.
- 林仕良, 丛峰, 高永娟, 等. 2012. 滇西腾冲地块东南缘高黎贡山群片麻岩 LA-ICP-MS 锆石 U-Pb 年龄及其地质意义 [J]. 地质通报, 31(2/3): 258–263.
- 刘琦胜, 叶培盛, 吴中海. 2012. 滇西高黎贡山南段奥陶纪花岗岩 SHRIMP 锆石 U-Pb 测年和地球化学特征 [J]. 地质通报, 31(2/3): 250–257.
- 刘一鸣, 李才, 王明, 等. 2014. 藏北羌塘盆地望湖岭组流纹岩地球化学特征及其地质意义 [J]. 地质通报, 33(11): 1759–1767.
- 刘志强. 2006. 西藏申扎永珠一带石炭—二叠系碎屑岩及其沉积环境探讨 [D]. 中国地质科学院硕士学位论文: 1–62.
- 罗安波. 2022. 班公湖—怒江洋消亡时限和过程——基于早白垩世沉积岩和火山岩的研究 [D]. 吉林大学博士学位论文: 1–232.
- 时超, 李荣社, 何世平, 等. 2010. 藏南亚东地区片麻状含石榴子石黑云花岗闪长岩 LA-ICP-MS 锆石 U-Pb 测年及其地质意义 [J]. 地质通报, 29(12): 1745–1753.
- 王保弟, 王立全, 王冬兵, 等. 2018. 三江昌宁—孟连带原—古特提斯构造演化 [J]. 地球科学, 43(8): 2527–2550.
- 王强, 赵振华, 熊小林. 2000. 桐柏—大别山带燕山晚期 A 型花岗岩的厘定 [J]. 岩石矿物学杂志, 19(4): 297–306.
- 王晓先, 张进江, 杨雄英, 等. 2011. 藏南吉隆地区早古生代大喜马拉雅片麻岩锆石 SHRIMP U-Pb 年龄、Hf 同位素特征及其地质意义 [J]. 地学前缘, 18(2): 127–139.
- 吴福元, 李献华, 杨进辉, 等. 2007. 花岗岩成因研究的若干问题 [J]. 岩石学报, (6): 1217–1238.
- 吴福元, 刘传周, 张亮亮, 等. 2014. 雅鲁藏布蛇绿岩——事实与臆想 [J]. 岩石学报, 30(2): 293–325.
- 吴昊, 翟庆国, 胡培远, 等. 2021. 西藏班戈北部早白垩世火山岩: 班公湖—怒江洋闭合的岩浆记录 [J]. 中国地质, 48(5): 1623–1638.
- 解超明, 段梦龙, 于云鹏, 等. 2019. 西藏松多地区早侏罗世变质辉长岩的成因及其构造意义 [J]. 岩石学报, 35(10): 3065–3082.
- 解超明, 李才, 翟庆国, 等. 2021. 藏北羌塘早古生代岩浆作用及其地质意义 [J]. 沉积与特提斯地质, 41(2): 340–350.
- 解超明, 李才, 苏黎, 等. 2010. 藏北安多地区花岗片麻岩锆石 LA-ICP-MSU-Pb 定年 [J]. 地质通报, 29(12): 1737–1744.
- 解超明, 李才, 王明, 等. 2014. 藏北聂荣微陆块的构造亲缘性——来自 LA-ICP-MS 锆石 U-Pb 年龄及 Hf 同位素的制约 [J]. 地质通报, 33(11): 1778–1792.
- 徐文坦, 张雪辉, 张斌斌, 等. 2022. 赣东北地区福泉山岩体高分异 S 型花岗岩成因: 来自锆石 U-Pb 年龄、Hf 同位素及地球化学的证据 [J]. 地质通报, 41(4): 577–589.
- 许志琴, 杨经绥, 梁凤华, 等. 2005. 喜马拉雅地体的泛非—早古生代造山事件年龄记录 [J]. 岩石学报, 21(1): 1–12.
- 杨学俊, 贾小川, 熊昌利, 等. 2012. 滇西高黎贡山南段公养河群变质基性火山岩 LA-ICP-MS 锆石 U-Pb 年龄及其地质意义 [J]. 地质通报, 31(2/3): 264–276.
- 负晓瑞, 蔡志慧, 何碧竹, 等. 2019. 西藏安多地区早古生代及中生代造山记录: 来自安多微陆块—南羌塘锆石 U-Pb 年代学及 Hf 同位素研究 [J]. 岩石学报, 35(6): 1673–1692.
- 张博川. 2021. 西藏物玛地区始新世流纹岩的岩石成因及地质意义 [D]. 吉林大学硕士学位论文: 1–51.
- 张洪亮, 杨文光, 朱利东, 等. 2019. 南拉萨地块高分异 S 型花岗岩锆石 U-Pb 年龄、地球化学特征及地质意义 [J]. 矿物岩石, 39(1): 52–62.
- 张亮亮, 朱弟成, 赵去丹, 等. 2010. 西藏北冈底斯巴尔达地区岩浆作用的成因: 地球化学、年代学及 Sr-Nd-Hf 同位素约束 [J]. 岩石学报, 26(6): 1871–1888.
- 张天羽. 2018. 青藏高原及邻区早古生代构造运动 [D]. 吉林大学博士学位论文: 1–133.
- 张泽明, 王金丽, 沈昆, 等. 2008. 环东冈瓦纳大陆周缘的古生代造山作用: 东喜马拉雅构造结南迦巴瓦岩群的岩石学和年代学证据 [J]. 岩石学报, 24(7): 1627–1637.
- 张雨轩, 解超明, 于云鹏, 等. 2018. 早侏罗世新特提斯洋俯冲作用—来自松多高镁闪长岩锆石 U-Pb 定年及 Hf 同位素的制约 [J]. 地质通报, 37(8): 1387–1399.
- 支倩, 任蕊, 段丰浩, 等. 2023. 西淮噶尔南部晚石炭世中—酸性火山岩成因机制及其对准噶尔洋闭合时限的约束 [J/OL]. 地学前缘, 31(3): 1–21.